

Aus dem Max-Planck-Institut für Neurobiologie, Abteilung Zelluläre und Systemneurobiologie  
Direktor: Prof. Tobias Bonhoeffer

## **The role of EphrinA for retinotopic map formation in mouse visual cortex – an Optical Imaging study**

Dissertation  
zum Erwerb des Doktorgrades der Medizin  
an der Medizinischen Fakultät der  
Ludwig-Maximilians-Universität zu München

vorgelegt von  
**Claire Creutzfeldt**  
aus Göttingen

2003

Mit Genehmigung der Medizinischen Fakultät  
der Universität München

Berichterstatter: Prof. Dr. med. U. Büttner

Mitberichterstatter: Prof. Dr. Th. Heinzeller  
Prof. Dr. J. Herms

Mitbetreuung durch die  
promovierten Mitarbeiter: Dr. Mark Hübener, Prof. Tobias Bonhoeffer

Dekan: Prof. Dr. med. Dr. h.c. K. Peter

Tag der mündlichen Prüfung: 27.November 2003

## Acknowledgements

Most of all, I want to thank **Mark Hübener** who faithfully and patiently supported me and helped me wherever he could. He taught me a great deal about imaging, about the visual cortex, and about science in general. Mark's enthusiasm and humour are very contagious and he stimulated my own thoughts and ideas and was great fun to work, discuss and laugh with.

I am indebted to **Sven Schütt** who laid the foundations for this project. Thanks in particular to his computer programming skills, I could step into the experiments right away.

The other essential originator of this project to whom I am very grateful, is **Lothar Lindemann**, who established this intriguing way of rendering mice deficient for all EphrinAs.

I want to thank **Tobias Bonhoeffer** for his advice on the project and for his help, both professional and personal, with the "what next?".

Many other lab members were of indispensable help, especially **Max Sperling** without whom I would not have been able to work my way through Sven's programmes, and **Martin Korte** for his helpful and inspiring ideas and for proof reading the manuscript.

All the members of the Bonhoeffer and Grothe labs together were responsible for a very pleasant and motivating atmosphere.

I want to thank **Ulrich Büttner** for reviewing this thesis.

My mother, **Mary**, and my twin sister, **Ruth**, as well as my sister **Corinna** and brother **Benjamin**, have been my most faithful and encouraging supporters throughout, just like **Armin**, who accompanied me from the beginning of my thesis and helped me not only over this mountain.

*to my father*

„The cortex is not a wishy-washy thing“  
(Otto Creutzfeldt)

# Contents

<b>1</b>	<b>Introduction.....</b>	<b>3</b>
1.1	Maps in the brain .....	3
1.2	Gradients of molecular labels .....	4
1.3	‘Eph’ receptors and ‘ephrin’ ligands.....	6
1.4	Ephrin-A5 knockout mice.....	8
1.5	Thalamocortical mapping .....	9
1.6	<i>In-vivo</i> functional imaging.....	9
1.7	Transgenic mice with a multiple ephrin-A deficiency.....	10
<b>2</b>	<b>Materials and Methods.....</b>	<b>13</b>
2.1	Surgery.....	13
2.2	Optical imaging.....	14
2.3	Analysis.....	15
2.4	Genotyping.....	17
<b>3</b>	<b>Results .....</b>	<b>18</b>
3.1	Retinotopic organisation of the primary visual cortex.....	19
3.2	Comparing maps in wild type and knockout mice.....	20
3.3	Quantitative characteristics of retinotopic maps in wild type and knockout mice.....	25
3.4	Retinotopic maps in young wild type and knockout mice.....	29
<b>4</b>	<b>Discussion.....</b>	<b>35</b>
4.1	The retinotopic map in the primary visual cortex of ephrin-A knockout mice is grossly normal.....	36
4.2	Adult ephrin-A knockout mice show a distortion in the map of the primary visual cortex .....	39

4.3	Mice lacking all ephrin-A ligands show a similar cortical phenotype as ephrin-A5 knockout mice. ....	41
4.4	Young ephrin-A knockout mice exhibit a stronger phenotype than adult mice. ...	45
4.5	Conclusion .....	46
	<b>Bibliography .....</b>	<b>48</b>
	<b>Summary.....</b>	<b>53</b>
	<b>Zusammenfassung (deutsch).....</b>	<b>54</b>
	<b>Curriculum Vitae .....</b>	<b>56</b>

# 1 Introduction

The cerebral cortex is the seat of our sensory, motor and cognitive abilities and in humans contains over 10 billion neurons. A deeper understanding of how it works, how it develops and how it is functionally organised may bring us further in understanding our own mental processes – how we feel, perceive and even think.

## 1.1 Maps in the brain

When looking more closely at the mammalian neocortex, one striking feature is the accuracy of its structural and functional organisation.

During development of the neocortex, distinct areas are formed, which are each characterised by their specific inputs, their intrinsic processing networks and by specific outputs. In many areas of the sensory cortex, this includes the formation of “topographic maps” meaning that there is a faithful transfer of spatially organised information from one region of the brain to another, so that neighbouring cells in the input structure are connected to neighbouring cells in the target region.

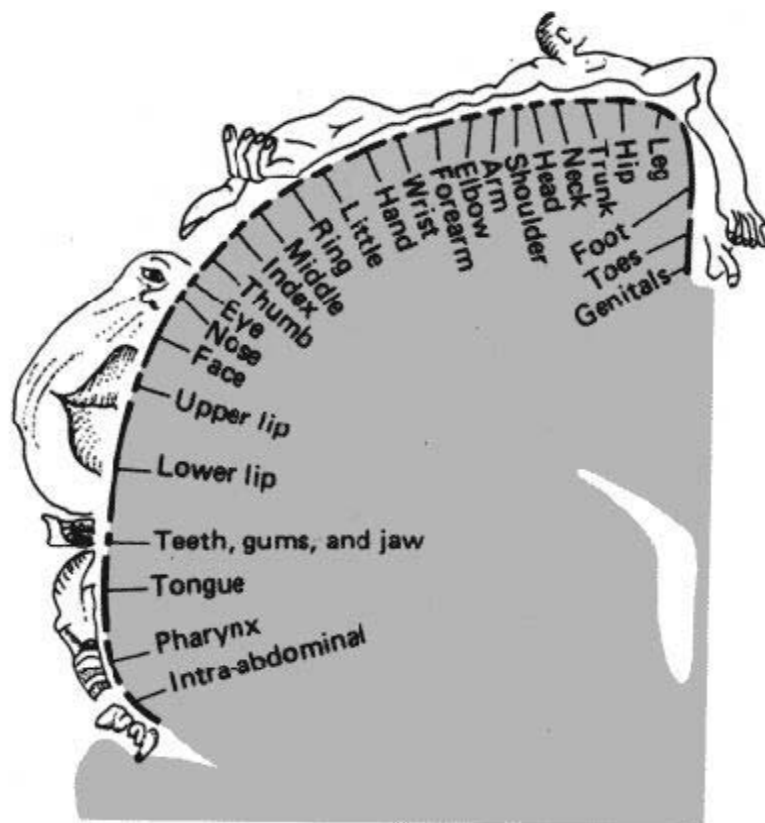
One prominent example of such a topographic map can be found in the primary somatosensory cortex (S1) where the entire body surface is represented by a precise map, the so-called “homunculus” (Figure 1). In this and many other maps, the cortical space devoted to a certain region reflects its functional importance, e.g., the “swollen” lips or large fingertips of the homunculus reflect the high density of touch receptors in the respective parts of the skin.

In a similar way, the primary visual cortex (Brodmann area 17) contains an ordered retinotopic map. Retinal axons project topographically to their targets in the brain, and this topography is maintained also on the level of the cortex. Thus, the spatial organisation of information received by the eyes is maintained upon transfer to the brain.

### **Figure 1 (see next page): Sensory homunculus**

The sensory homunculus depicts the representation of the sensory periphery in the somatosensory cortex. Note the overall continuous representation of the body surface. The map is distorted since, based on differences in the density of touch receptors, individual body parts occupy different amounts of cortical space. Fingers, face and mouth look swollen, while upper arm and torso are unproportionally small.

(Adapted from Penfield and Rasmussen, (1950))



## 1.2 Gradients of molecular labels

But how, during development of the nervous system are these precise neuronal connections established? In other words, how do outgrowing axons know where to go?

The prevailing hypothesis for the mechanism of topographic map formation was proposed by Roger Sperry already decades ago (Sperry, 1943). He suggested that axonal connections are determined by “individual identification tags, presumably cytochemical in nature” that guide the axons through their environment to ultimately reach their target neuron. Further, his ‘chemoaffinity’-theory postulates the presence of complementary cytochemical gradients on retinal axons and their target regions in the brain. The axonal growth cones, which are equipped with chemical sensors themselves, read this surface-associated information and grow, according to their affinity, along the concentration of specific guiding molecules.



To test this hypothesis, a method had to be developed to detect this preference of growing axons for certain membrane-bound markers and their concentrations and, thus, for the correct position in the brain.

A breakthrough in this search was the development of the *in-vitro*-stripe-assay (see Figure 2) where retinal axons (in this case: chick retinal axons), their normal target area being the optic tectum, are allowed to choose between alternating stripes of membrane vesicles derived from anterior or posterior tectal cells (Walter et al., 1987). It was in fact shown that fibres from the temporal part of the retina, which normally terminate in the anterior part of the tectum, grew preferentially on anterior tectal membranes. This behaviour was demonstrated to be caused by a repellent activity associated with the posterior membranes. In contrast, according to (Feldheim et al., 1998), nasal axons showed no consistent preference, the posterior membranes being their natural target.

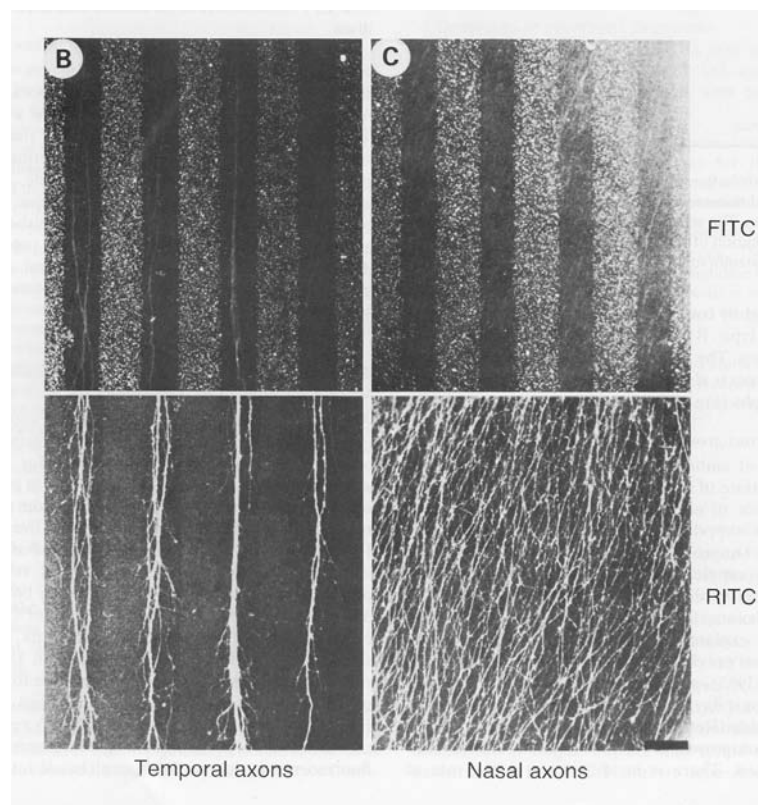


**Figure 2: *In-vitro* stripe assay**

A retinal explant has been placed on a striped carpet with membranes from either anterior (dark stripes) or posterior (light stripes, coloured with green fluorescence dye, FITC) tectal cells. Panel B shows typical growth patterns of temporal, panel C those of nasal axons after 2 days in culture. The lower panels show the distribution of the RITC labeled retinal axons. While nasal axons show no preference for one type of stripes, temporal axons grow preferentially on the stripes of anterior tectal membranes. Scale bar 100  $\mu$ m. Taken from Walter et al. (1987).

### 1.3 ‘Eph’ receptors and ‘ephrin’ ligands

Several cell surface molecules were subsequently identified and since then, strong evidence has been provided for their function as topographic labels. The first hints for an involvement of the so-called Eph receptor tyrosine kinases and their ligands, the ephrins, came from two reports: two closely related molecules, later termed ephrin-A2 and ephrin-A5, were hypothesised as guidance molecules for retinal ganglion cell (RGC) axons, showing graded expressions in the optic tectum and thalamic nuclei and axon repellent activity (Cheng et al., 1995; Drescher et al., 1995).

Subsequently, the structure and function of Eph receptors and their ligands have been studied in great detail. They are now known to be widely expressed in the brain and to have important roles in many developmental phenomena, ranging from axon guidance and cell migration to vascular development (O’Leary and Wilkinson, 1999).

Based on sequence similarities, Eph receptors are subdivided into EphA and EphB receptors. The eight known ephrin ligands are anchored to the membranes in two different ways, the A-subfamily by a glycosyl phosphatidylinositol (GPI) linker, and the ephrin-Bs by a transmembrane domain. Within each receptor-ligand subfamily, there is a high degree of binding promiscuity (Figure 3). However, an individual Eph receptor has a wide variation in affinity for different ephrins.

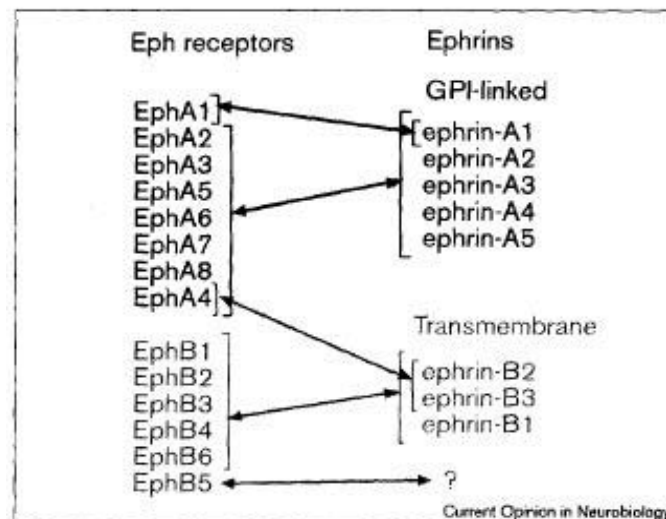


**Figure 3: Family tree and binding specificities of the Eph receptor and ephrin families**

The Eph family contains at present 14 different receptors and 8 ligands, which are subdivided into 2 classes: the EphA subclass containing GPI-anchored ephrin-A's interacting mainly with EphA receptors and the EphB subclass with transmembrane anchored ephrin-B's interacting with a complementary set of EphB receptors. Some ephrin-B ligands have also been shown to bind to EphA receptors (O’Leary and Wilkinson, 1999).

Gene expression and functional studies indicate that these molecules might be involved in the formation of many different topographic maps, including projections from retina to tectum (Cheng et al., 1995), retina to thalamic nuclei (Feldheim et al., 1998), hippocampus to lateral septum (Gao et al., 1996) and thalamus to cortex (Vanderhaeghen et al., 2000; Gao et al., 1998).

*In situ* hybridisation showed counter gradients for Eph receptors and their ligands in the developing chick retina and in the tectum (Cheng et al., 1995). EphA3, the preferred receptor of ephrin-A2 and A5, and its cousins, EphA4 and EphA5, are expressed in a high temporal to low nasal gradient by RGCs. Complementary to this, both ephrin-A2 and A5 show an increasing anterior-posterior (A-P) gradient in the tectum, the former being present in a smooth gradient across the entire tectum, whereas ephrin-A5 seems to be confined to the posterior half of the tectum and exhibits a steeper gradient (Figure 4).

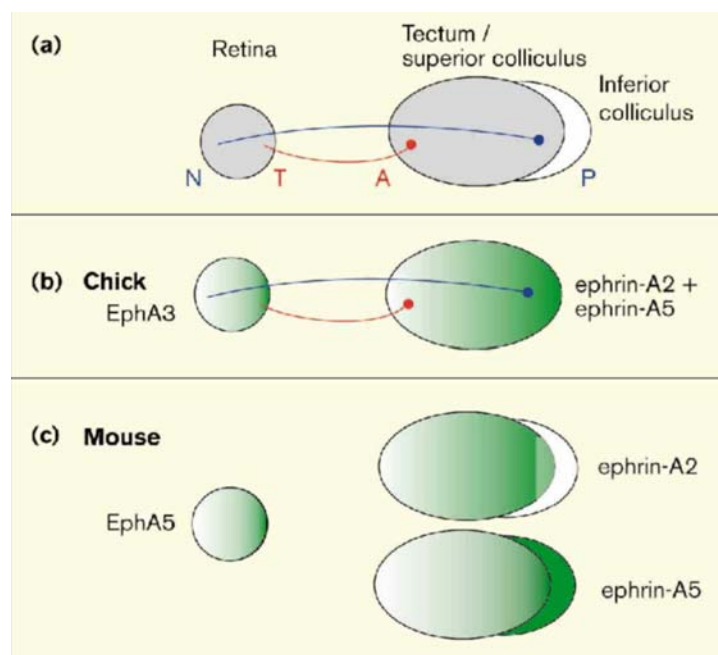


**Figure 4: Topographic mapping and EphA/ephrin-A expression**

The retinotectal projection is a well-characterised system serving as a model for topographic projections. a) Retinal axons form a map in which temporal axons (T) project to the anterior (A), and nasal axons (N) to the posterior (P) tectum (or to its mammalian equivalent, the superior colliculus). b) In the chick retina, EphA3 is expressed in a gradient that is complementary to that of ephrin-A2 and A5 in the tectum. c) In the mouse, there is graded expression of EphA5 (rather than of EphA3) in the retina, and of ephrin-A2 and A5 in the superior colliculus. Ephrin-A5 is also expressed in the inferior colliculus, one of the auditory relay and reflex centres (Wilkinson, 2000).

RGCs with low levels of EphA3 map to parts of the tectum with high levels of ephrin-A2 and A5, and vice versa. The obvious interpretation of this finding is that ephrin-A2 and A5 act as repellents for temporal RGC axons.

In the lateral geniculate nucleus (LGN), the visual relay station in the thalamus that projects to the primary visual cortex, retinal fibres terminate in a topographic order as well. Also here, ephrin-A2 and A5 are expressed in gradients that match the nasotemporal ordering of retinal fibres (Feldheim et al., 1998).

#### **1.4 Ephrin-A5 knockout mice**

The effects of EphA receptors and their ligands on topographic map formation and RGC axon guidance have been determined by both *in-vitro* (Feldheim et al., 1998) and *in-vivo* (Nakamoto et al., 1996) functional assays, mostly in the nervous system of the chick. The next logical step was to study their role by *in-vivo* loss-of-function analysis in mice with targeted gene deletions.

In the murine nervous system, ephrin-A ligands are expressed in the embryonic superior colliculus (SC) in a low anterior to high posterior gradient (Zhang et al., 1996), with ephrin-A5 showing a smooth gradient across the entire SC, similar to ephrin-A2 in the chick tectum. In addition, ligand-binding activity indicates a high temporal to low nasal gradient of EphA5 receptors (Feldheim et al., 1998), most likely serving the same function as EphA3 in the chick retina.

Axonal tracing in mice lacking ephrin-A5 reveals substantial aberrancies in the topographic organisation of the retinocollicular projection (Frisen et al., 1998). In these mice, temporal RGC axons (with high EphA5) arborise ectopically in posterior SC, where ephrin-A5 would normally be expressed at high levels, and thus act as an axonal repellent. However, RGC axons do also show dense arborisations at the topographically correct sites, suggesting that other molecules, ephrin-A2 for example, compensate in part for the lack of ephrin-A5. Further, in the absence of ephrin-A5, there is an increase of retinal axons that initially overshoot the superior colliculus (SC), extending into the inferior colliculus (IC), which is an auditory relay station and thus normally never innervated by RGCs. This is consistent with a barrier function for ephrin-A ligands, in order to prevent neuronal growth cones from growing into inappropriate territories.

In double ephrin-A2/A5 homozygous mutants, the retinocollicular anterior-posterior topography is even less discernible and there are even more anterior projections of

nasal axons than in the ephrin-A5 single mutant (Feldheim et al., 2000). Surprisingly, the projections of retinal axons still fill the superior colliculus, rather than there being a complete overshoot.

Also in the LGN, ephrin-A5 knockout mice clearly show mapping abnormalities with nasal axons forming wider, less dense and slightly shifted arborisations, and temporal axons showing a second smaller arborisation in addition to the expected one (Feldheim et al., 1998).

### **1.5 Thalamocortical mapping**

The studies described above have established the influence of Eph receptors and their ligands on axon path finding in the development of the retinocollicular and retinothalamic projections and thus their role in establishing the correct connections between retina and midbrain and between retina and forebrain.

Studies in recent years suggest a similar role of these molecules for the development of topographic maps in the neocortex (Gao et al., 1998). *In situ* hybridisation for EphA RNA showed graded expression of EphA5 in the murine thalamus. Ephrin-A5 is expressed in a prominent high medial to low lateral gradient across the somatosensory cortex, S1. Complementary to this finding, the thalamic VB (ventrobasal) complex, the main somatosensory relay station to the cortex, displays an EphA4 receptor gradient (high ventromedial to low dorsolateral). Importantly, VB axons were differentially repelled by ephrin-A5 *in vitro* (Vanderhaeghen et al., 2000).

### **1.6 *In-vivo* functional imaging**

To test whether ephrin-A5 affects the functional organization of the cortex *in vivo*, Prakash and colleagues (2000) mapped cortical areas using optical imaging of intrinsic signals (Grinvald et al., 1996).

Similar to the *in vitro* findings of Vanderhaeghen and colleagues, the map of the barrel cortex, the part of the primary somatosensory cortex where every single whisker is represented individually, was grossly normal in ephrin-A5 knockout mice (Prakash et al., 2000). However, moderate distortions in barrel sizes were observed, with a contraction of barrels medially (where ephrin-A5 is normally expressed at high levels) and a map expansion laterally. This medial shift in thalamocortical axon termination zones, toward the region with usually high levels of repellent ligands,

would fit to the idea that ephrin-A5 might act as a complementary within-area mapping label for somatosensory thalamocortical axons.

However, optical imaging of the barrel cortex has the great disadvantage that, in order to image the complete map, every single whisker would have to be stimulated individually.

I chose the visual modality for various reasons. Classically, the retinofugal system has been the popular model system for the study of topographic projections. As we have just learned, much is already known about the nature of the projections from retina to brain, and a number of molecular gradients have been revealed in the retina and its targets, i.e. the tectum, the thalamus and also in the visual cortex itself. Further, the visual system is ideally suited to map the entire sensory surface because a large part of the visual field can be easily stimulated. Moreover, due to its small size, the whole visual cortex, and not only the primary visual area, can be mapped within a single imaging session.

Using this method, Sven Schuett in this lab was able to map mouse visual cortex very precisely (Schuett et al., 2002). The maps obtained with optical imaging corresponded exactly in position, size and shape to area 17 as seen in stained histological sections.

Subsequently, Schuett and his colleagues applied this method to ephrin-A5 knockout mice. Here, a change could be demonstrated in the ordered retinotopic map in area 17, showing a compression of the cortical representation of the visual periphery and, more generally, an increase in the variability of patch position compared to wild-type mice (Hübener et al., 2001).

Thus, optical imaging of mouse visual cortex seems to be a very suitable way to screen genetic factors controlling topographic mapping in the neocortex.

### **1.7 Transgenic mice with a multiple ephrin-A deficiency**

Summarising the above results, ephrin-A5 has been shown to act as a developmental anteroposterior guidance label for both the retinotectal/retinocollicular and retinothalamic projection, and it is also involved in the formation of topographic maps in the neocortex. In each station along the visual pathway, the tectum, the LGN and the cortex, mice lacking this ligand show a distorted map topography. The phenotype of the retinocollicular projection in mice lacking both ephrin-A5 and ephrin-A2 is yet more severe than in either single mutant (Feldheim et al., 2000). However, a

topographic bias remains even in the double mutant, suggesting additional factors that are able to compensate for the loss of ephrin-A5 and ephrin-A2 to a certain extent.

The detailed roles of other ephrins in the visual system are yet to be determined. As described earlier, at least two other related receptors besides EphA3 are expressed in RGCs, EphA4 and EphA5. Various EphA receptors are also expressed in the tectum, and some ephrin-A ligands are expressed in the retina (Flanagan and Vanderhaeghen 1998). Almost all the receptors are expressed in the developing or adult nervous system (Tuzi and Gullick, 1994). Altogether, the results suggest a considerable degree of functional redundancy, which is consistent with the high degree of binding promiscuity within this family of axonal guidance cues.

To fully test the importance of the entire ephrin family for mapping in the visual system one would ideally like to have a multiple ephrin-A knockout mouse. In other words: What consequences would it have for the topographic organisation of the retinotopic map if one ephrin-A could not compensate the deficiency of another?

Unfortunately, the generation of such a multiple knockout mouse is very difficult and laborious. In an alternative approach, Lothar Lindemann in the lab of Yves Barde at the Friedrich-Miescher Institute in Basel has developed a “knock-in” mouse that is aimed to be deficient of all ephrin-As in the nervous system (Lindemann, 2001). In this mouse, a cDNA, coding for a so-called receptor body, was targeted into the tau-locus of the genome. This receptor body is secreted by neurons and consists of the extracellular domain of the EphA5 receptor and the Fc part of human IgG1. The tau-locus was chosen for various reasons: tau is expressed early (from approx. E 9.5-10.0) and strongly, and it persists into adulthood. Further, it is specific for neurons and its absence has been shown not to influence nerve growth (Tucker et al., 2001). Because of the high degree of binding promiscuity within each receptor-ligand subfamily, the receptor body can bind and thereby block all ephrin-As. In effect, this mouse is a functional all ephrin-A deficient animal. The mice were termed TIBFmyc mice, because the construct coding for the receptor body fusion protein was (in the following order starting at the N-terminus) targeted to the tau-locus (T); it consists of the Ig-kappa signal peptide (I), which enables the protein to be secreted; B stands for the extracellular domain of the EphA5 receptor and is derived from the old nomenclature BSK; the FC-part of human IgG (F) was chosen as it causes a dimerisation of two protein molecules, thus increasing the affinity to the ephrin ligands. Finally, the myc-tag was added on to the c-terminus to enable the detection of

the protein through various already known myc-antibodies. For the sake of simplicity, I shall from now on be referring to these mice as knockout mice, although I am well aware that they are not proper genetic but merely functional ephrin-A knockout mice. The aim of my thesis was to map the visual cortex in these mice with optical imaging of intrinsic signals to gain a better understanding of the role of ephrins for topographic mapping in the neocortex. As controls, wild type mice and mice heterozygous for the functional defect were also imaged.

Since it is conceivable that initial mapping defects caused by the lack of ephrin-As are compensated during later stages of development by factors such as neuronal activity or simply time, I also performed experiments with mice of around two weeks of age, which is about the earliest possible age for optical imaging in mice (see Figure 5).

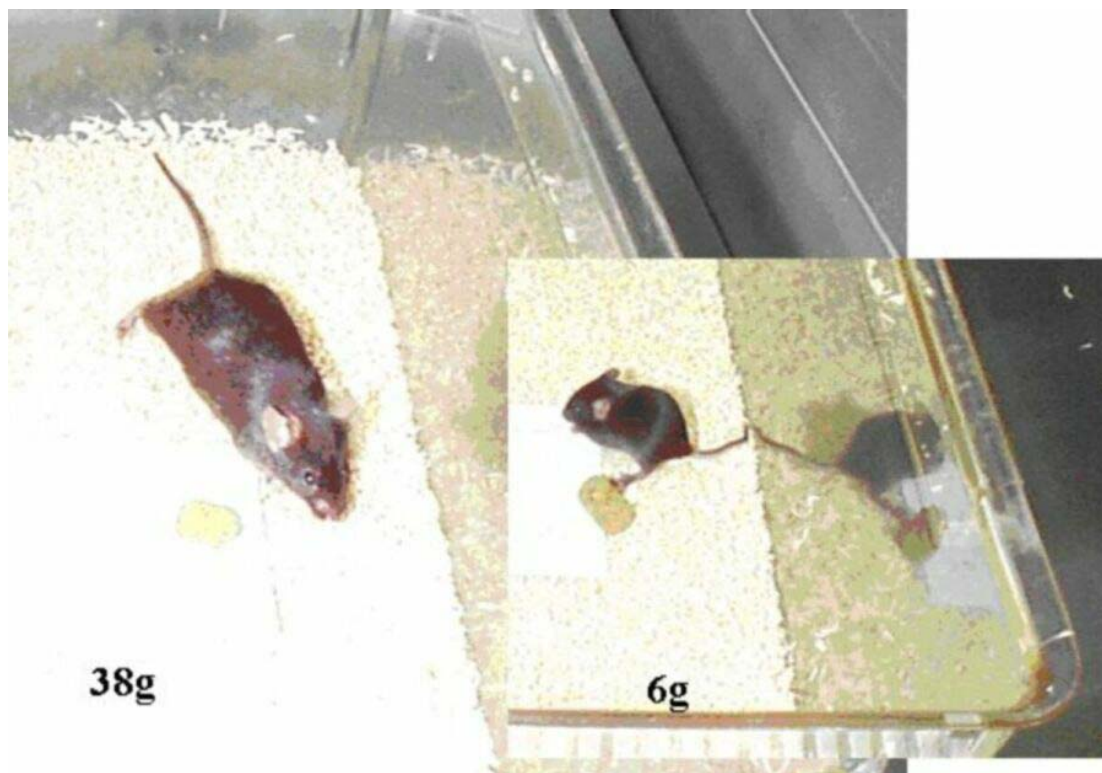


**Figure 5: Comparing size and weight of adult and young mice**

These images illustrate the size and weight difference between adult and young mice used in this study. The first set of experiments was carried out on adult mice, aged approx. 7-10 months, with a weight of around 40g. Subsequently, young mice were imaged of around two weeks of age that weighed no more than 10g.



## **2 Materials and Methods**

The first set of experiments was carried out on 14 adult mice of 7-10 months of age. I used mixed background C57BL/6 x SV/129J mice, 5 of which were wild type, 4 heterozygous and 5 functional knockout mice.

The second set was performed on 8 young mice (P 14-16) of mixed background, 4 wild type and 4 functional knockout mice.

Throughout the imaging experiment and the essential part of the data analysis I was blind to the mouse genotype. The mice had been given an identification number and were coded by ear punching. After each experiment, a tail biopsy was performed in order to later analyse the genotype.

The methods described here were essentially established by Schuett and colleagues (Schuett et al., 2002) in part altered and optimised. All procedures were carried out in accordance with local government rules and the guidelines of the Society for Neuroscience.

### **2.1 Surgery**

During a 30 second ether anaesthesia, a combination of urethane (500-600 mg/kg body weight i.p.) and ketamine (30-40 mg/kg body weight i.m.) was injected for initial anaesthesia. This was maintained with a continuous i.p. infusion of 15 mg/kg body weight ketamine and 10mg/kg body weight urethane.

In order to inject young mice ( $\leq 10$ g), they were put into an induction chamber, which was slowly filled with 2% halothane in air and then injected with 300 mg/kg body weight urethane and 30mg/kg ketamine i.p.

In most experiments, a small tubing was attached to the nose and the animals were respirated artificially (150-170 cycles/min). In these cases anaesthesia was additionally maintained by approx. 0.2 % halothane in a mixture of 70 % O<sub>2</sub> and 30% N<sub>2</sub>. The heart rate was continuously monitored and the depth of anaesthesia was adjusted to maintain a rate of 300-450 beats per minute. If a mouse breathed on its own, this was assisted by a continuous flow of oxygen to its nose.

The combination of anaesthetics was found to be crucial for reproducible high quality imaging and long-term stability of physiological conditions. In particular, to reliably image retinotopic maps, the pupils should not be dilated by the anaesthetics or other drugs.

A mixture of 35% glucose and 65% saline was infused i.p. at 0.3 ml/h (adult mice) and 0.1 ml/h (young mice) to prevent dehydration.

During surgery, the eyes were covered with eye protection cream (Isopto-Max, Alcon Thilo, Germany), which was replaced by silicon oil during optical imaging to prevent drying of the cornea.

The animal was initially positioned stereotaxically using mouth and ear bars, with the mouth bar positioned 3 mm below the inter-aural line (2 mm for the young mice). The skin above the skull was cut open and a few drops of silicon oil were immediately applied to the bone to maintain its transparency. The skull was then attached to a head holder with a mixture of glass beads and tissue glue (Histoacryl, Braun, Germany), and the mouth and ear bars were removed.

With the above procedures, I was able to record optical signals for well over 12 h in adult mice and for 6-12 hours in young mice.

The projection of the optic disc was determined in adult mice and was found to vary only little between animals (elevation:  $+ 32.7^\circ \pm 1.5^\circ$  SEM; azimuth:  $55.0^\circ \pm 2.0^\circ$  SEM;  $n = 6$  eyes from three mice).

## **2.2 Optical imaging**

A curved, transparent plastic screen was positioned in front of (13 cm distance) and lateral to (15 cm) the mouse. The screen covered the visual field in horizontal dimension from about  $-50^\circ$  to  $120^\circ$  measured relative to the vertical midline and between about  $-55^\circ$  to  $+20^\circ$  relative to the optic disk projection in vertical dimension. Visual stimuli were back-projected onto this screen with a video beamer. I stimulated at several positions in the visual field using moving square wave gratings, which changed their orientations randomly every 0.6 s (spatial frequency: 0.04 cycles/deg, speed: 2.5 cycles/second). These square shaped stimuli with  $25^\circ$  side length were presented in a random fashion at adjacent positions (7 columns and 3 rows of stimuli for the contralateral eye). Each six-second-stimulus presentation at one position was followed by a blank screen for eight seconds. To maximise the on-response I stimulated with a minimal luminance of  $1.25 \text{ cd/m}^2$  (maximal luminance:  $205 \text{ cd/m}^2$ ) for blank screen and background intensity.

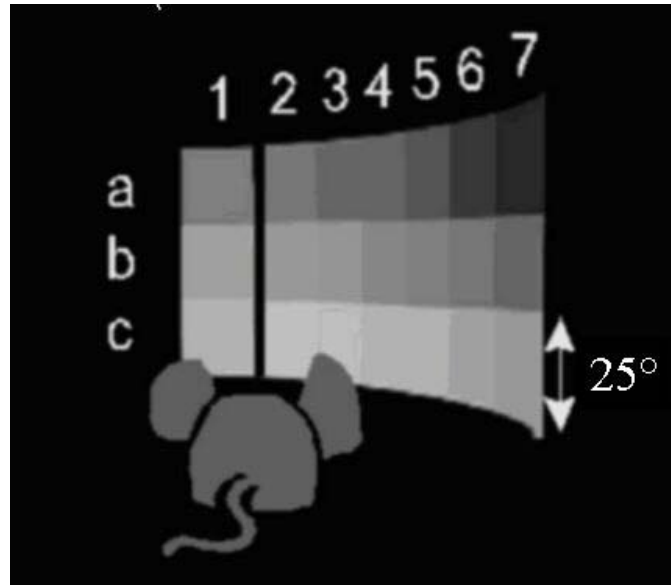


**Figure 6: Schematic of the experimental setup**

The mouse was positioned in front of a curved screen. Moving square wave gratings with 25° side length were presented in 3 rows (a,b,c) and 7 columns (1-7).

In nine experiments with adult mice, computer-controlled shutters allowed independent stimulation of the ipsi- and contralateral eye. In all other experiments, including those on young mice, only the contralateral eye was stimulated.

The cortex was illuminated with monochromatic light of 707 nm wavelength. Images were captured using a cooled slow-scan CCD camera (ORA 2001, Optical Imaging, Germantown, NY), focused 700  $\mu\text{m}$  below the cortical surface. Four “first-frames” (Bonhoeffer and Grinvald, 1996) and 10 frames of 600 ms duration were collected immediately before and during each six-second-stimulus presentation, respectively.

The imaged cortical region was chosen based on the superficial blood vessel pattern, the sagittal sinus forming the medial boarder of the imaged region and the transverse sinus crossing the image in the lower half.

### 2.3 Analysis

All images were “first frame-corrected”, i.e. from each image stack obtained during presentation, the four “first frames” taken immediately before stimulus presentation were subtracted. The resulting images were blank-corrected by subtracting the images acquired without stimulus from all images. In addition, the images were processed by a blood vessel extractor to remove blood-vessel-related artefacts. This method significantly improved the quality of the data and it clearly increased the inter-trial correlation, indicating a higher signal-to-noise ratio (Schuett et al., 2001). Twelve-bit

digitised camera data were range-fitted such that for the single condition maps the 1% or 3% most responsive pixels (least responsive pixels) of the entire set of images were set to black (white) for all DC-corrected or high-pass filtered images, respectively. To avoid erroneous DC correction due to large activated areas, which will slightly increase the mean of the intrinsic signal, each image was corrected for DC-shift using the mean of only those pixels, which varied less than one standard deviation (SD) of the blank response from its mean.

For quantification and alignment, all images were low-pass filtered with a Gaussian kernel of 99  $\mu\text{m}$  half width.

The region of the primary visual cortex was determined by thresholding the maximum intensity projection of the intrinsic signal, i.e. the light absorption, 2.5 SD of the blank response above the mean of the blank. In some cases, extrastriate areas lateral of area 17 had to be excluded by hand. The position of these lateral areas could be easily delineated both by shape and intensity. All subsequent computations were fully automated.

Both for averaging of single condition maps across animals and for quantification, all sets of single condition maps imaged in different animals were aligned using the eight most prominent patches (corresponding to stimuli 2-5 in rows b and c, see Figure 8A) elicited by visual stimulation as reference points to determine translation and rotation parameters. Patch position was defined by the centre of mass of the intrinsic signal in the primary visual cortex after thresholding the map 2.5 SD above its mean.

To visualise the overall retinotopic organization across the cortical surface, visual field position was colour-coded: in the “peak position projection”, each pixel was assigned the colour corresponding to the stimulus eliciting the strongest response at this pixel. Because of this “winner takes all” algorithm, the peak position projection contains distinct borders between cortical regions responding preferentially to different stimuli. To mask regions without a cortical response, colour saturation was chosen to code for the maximum intensity projection of the intrinsic signal across every activity patch.

These coding schemes can be applied to illustrate the retinotopic organisation of the excitatory response.

## 2.4 Genotyping

Immediately after birth, the mice were assigned an identification number and marked with that number by ear punching. Thus, each mouse can be easily identified by decoding the marking scheme and, at the same time, the experimenter is blind to the genotype in order to avoid any bias during both the experiment and analysis of the data.

In order to verify the genotype, a 3-5 mm tail biopsy was taken at the end of each experiment and stored at  $-20^{\circ}\text{C}$ .

Later, DNA was extracted from the tails in order to perform a polymerase chain reaction (PCR) with specific primers. I used all three primers (TKO2U5 = CATGGTGTCCCTTTCCCTTAC for wild type mice, Neo U3 = GATTCGCAGCGCATCGCCTTC for homozygous knock-in mice and genotIBFmyc D2 = CCCTCTTGTCAGCTCCTG, the universal primer, for heterozygous mice) in a single reaction.

The genotype was then identified by electrophoresis (see Figure 7). Wild type mice showed a band at 1.1kb, homozygous knock-in mice showed one at 0.65kb and those with two bands were heterozygous animals.

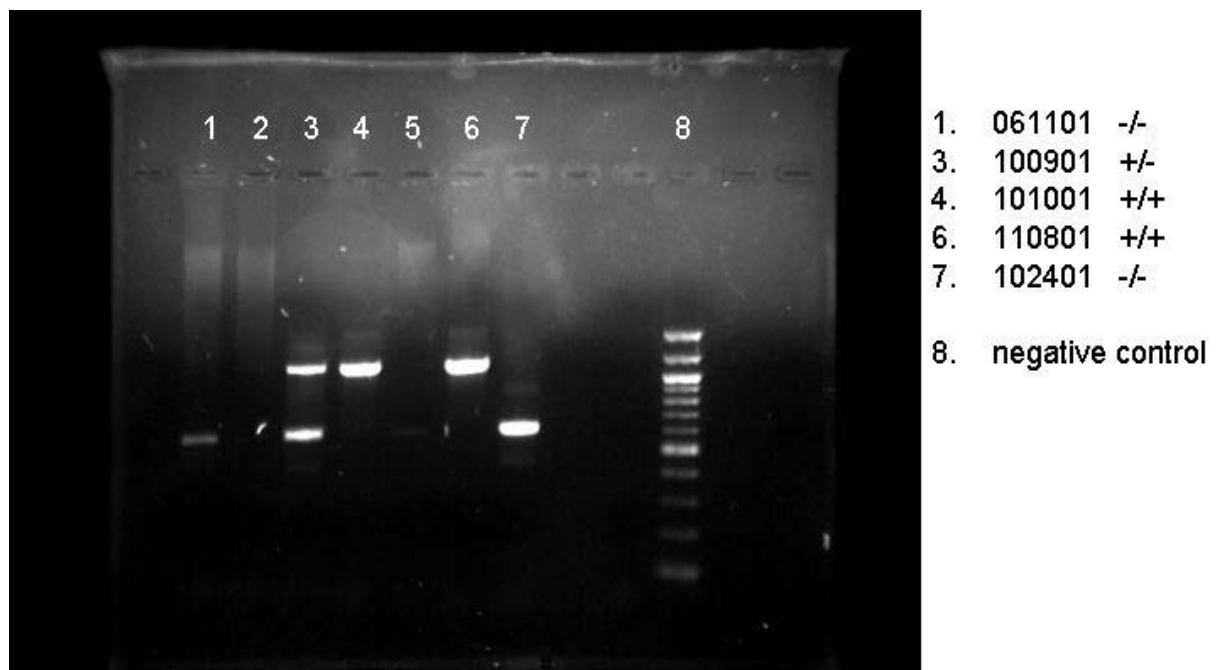


**Figure 7: Genotyping example**

The wild type allele has a fragment of approximately 1.1kb (upper band) the knockout allele one of approximately 0.65 kb (lower band). In heterozygous mice, both bands are visible.

### 3 Results

As described in the introduction, retinal ganglion cells project to their targets in the brain in a topographic fashion, neighbourhood relationships between neurons being thus maintained along the visual pathway. Assuming this order is continued all the way to the primary visual cortex, we should therefore expect to see an ordered retinotopic map across the entire area 17. In the next paragraph, I shall describe that this map can in fact be visualised with optical imaging of intrinsic signals.

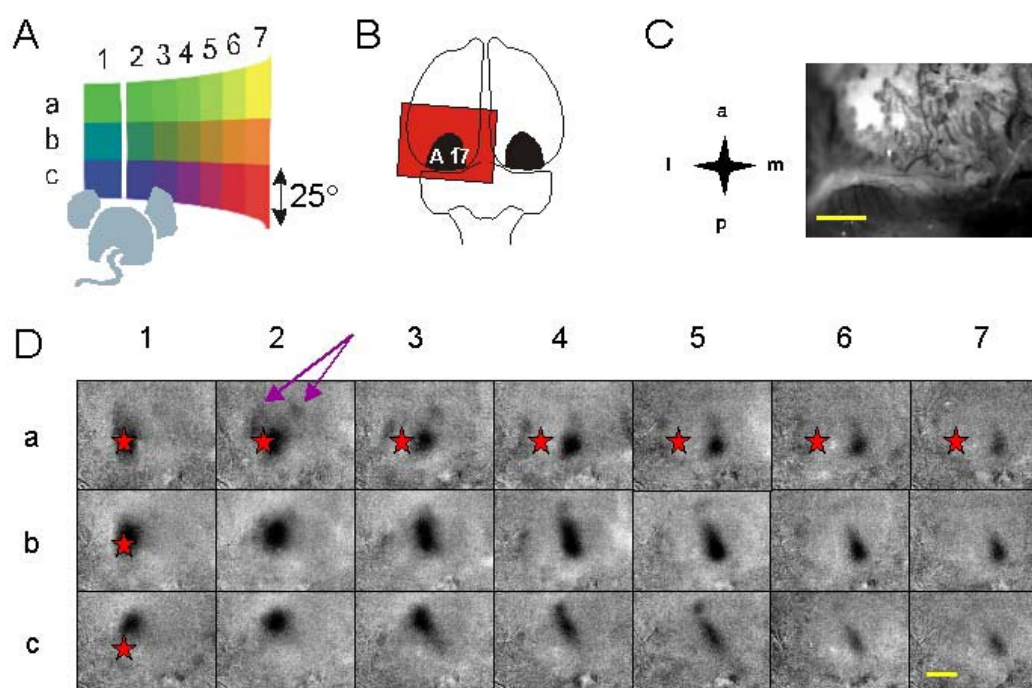


**Figure 8: Imaging retinotopic maps in mouse visual cortex**

- A The mouse is located in front of a curved screen and is successively stimulated with 21 square shaped stimuli (25 deg side length) presented randomly at adjacent positions in the visual field. The colour code representing stimulus position was used to generate colour-coded retinotopic maps (see Figure 9).
- B Scheme of the mouse brain with the medulla and the cerebellum visible at the bottom, followed rostrally (top) by the two cerebral hemispheres. The imaged region is indicated by the orange window, which contains a rough outline of area 17 (black patch).
- C Image of the blood vessel pattern obtained through the translucent skull. The left hemisphere was imaged; rostral is at the top, caudal at the bottom. The sagittal sinus (located between the two hemispheres) is on the right and continues further downwards and to the left into the transversal sinus. Area 17 is situated in the centre of the image. Scale bar: 1mm.
- D Blank corrected retinotopic maps from one wild type mouse. Each map corresponds to one stimulus position, as shown by the schematic in Figure 8A. For example, with the visual stimulus shown in position a1 (green), the map a1 is recorded. The dark patch in each map indicates the activated region in area 17, and occasional smaller patches reflect activity in extrastriate visual cortex (purple arrows). The red star indicates the position of patch a1 in every map and thus illustrates the progression of patches according to changes in stimulus position. Scale bar: 1mm.

### 3.1 Retinotopic organisation of the primary visual cortex

Every single visual stimulus (Figure 8A) induces a prominent patch of activity in the visual cortex (Figure 8D). Each of these patches is adjacent to (and at the same time largely overlapping with) the patch corresponding to an adjacent visual stimulus. From map to map, the activity patch changes its position from lateral to medial with different stimuli placed along the horizontal axis and the patch moves in an anterior-posterior direction in the cortex with changes of the stimulus position in the vertical dimension. The change in position of the patch is illustrated in Figure 8D by the red star, which indicates the position of the patch elicited by stimulus position *a1*. This demonstrates that, with the stimulation paradigm described above, we can image an ordered retinotopic map from the primary visual cortex.

Each principal dark patch is partly surrounded by a white halo. This increase in light reflectance has been shown to correspond to a reduction of the intrinsic signal below baseline and is the optical correlate of lateral inhibition (Schuett et al., 2002).

Further, we can observe smaller dark patches in one or several extrastriate cortical areas (see purple arrows in Figure 8D). These extrastriate areas are visible only in some of the single condition maps and they often lack a clear retinotopic organisation. To illustrate the overall retinotopic organisation of area 17, the stimulus positions were colour-coded (see Figure 9). The colour of each pixel within this map corresponds to the stimulus position, which elicited the strongest signal at this pixel.

As colour saturation equals the maximum intensity projection of all single condition maps, regions without activation remain dark. The multicoloured image demonstrates the continuous retinotopic progression within area 17, both in the horizontal and vertical dimensions, consistent with the different positions of the visual stimuli.

Since the intrinsic signal strength in extrastriate areas is much smaller than in the primary visual cortex, these areas are not visible in this map.

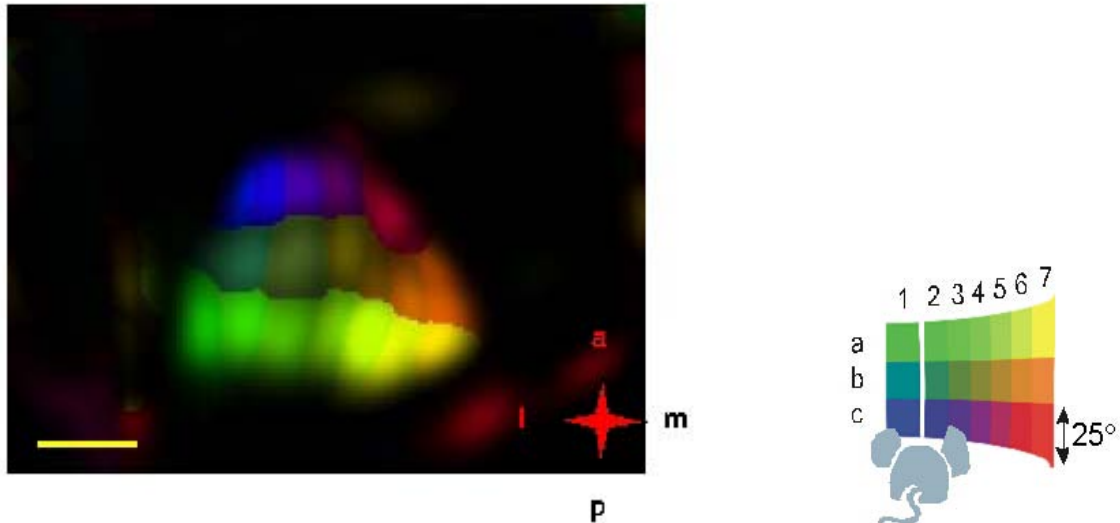


**Figure 9: Colour-coded retinotopic map of area 17**

The multicoloured image represents the primary visual cortex, with each colour corresponding to the stimulus position (see schematic on the right), which elicits the largest response at this point in the cortex. Thus, the continuous retinotopic progression consistent with the positions of the visual stimuli is revealed. l=lateral, m=medial, a=anterior, p=posterior. Scale bar: 1mm.

### 3.2 Comparing maps in wild type and knockout mice

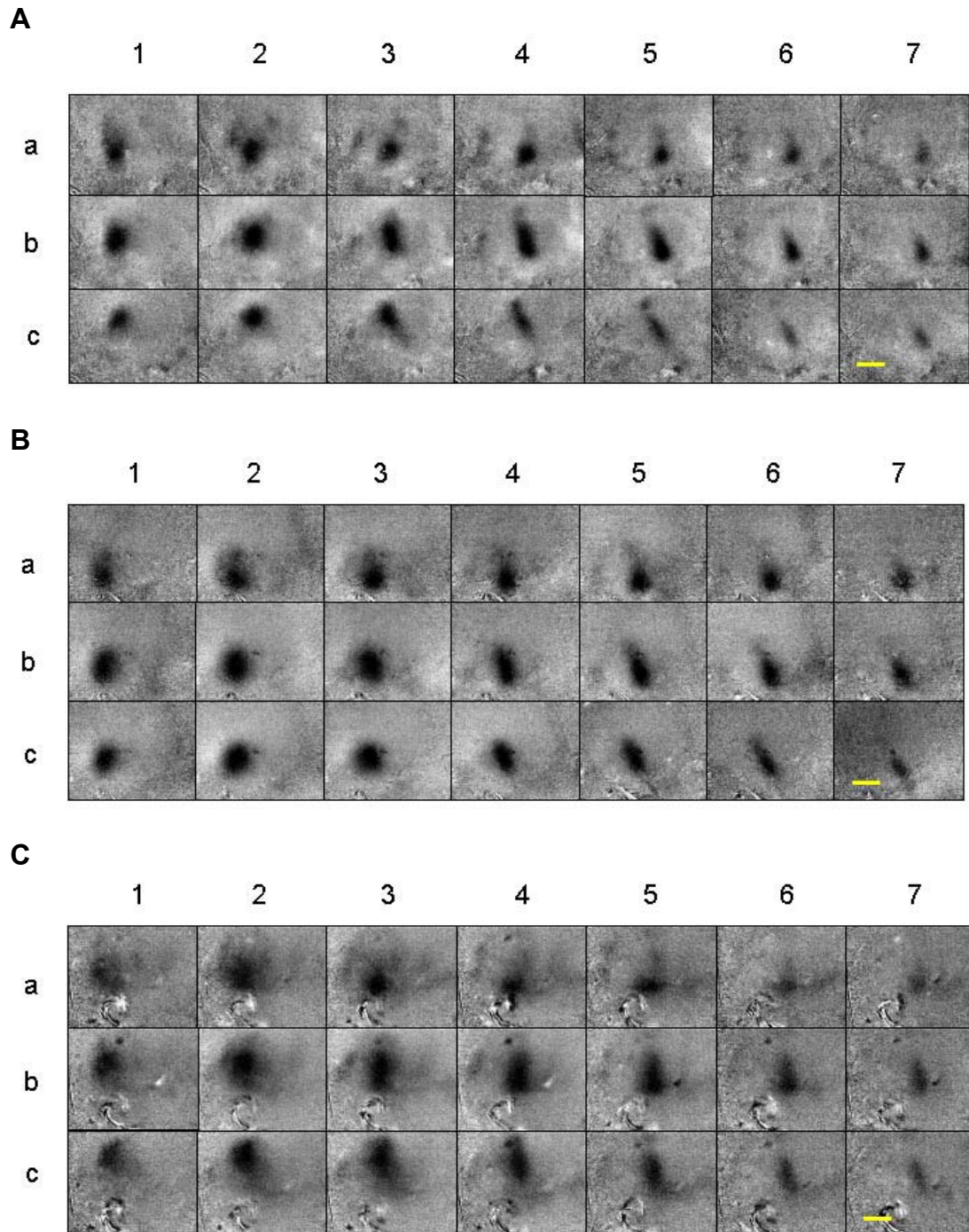
As the position of activity patches can be determined with high precision, these measures are well suited to compare the layout of topographic maps in the functional ephrin-A knockout mice with those obtained from wild type mice.

Figure 10 shows retinotopic maps obtained from a wild type (A), a heterozygous (B) and a knockout (C) mouse.

Again, we can see the activity patch in every retinotopic map and follow its progression within area 17. Let us focus on the central patches corresponding to stimuli 2-4 in rows a, b and c (see Figure 8A):

A comparison of the retinotopic maps of these three mice reveals, that, even in the functional knockout mouse, there exists a retinotopic organisation in the primary visual cortex. Thus, on this level of analysis, functional blockade of ephrins does not seem to grossly disturb the formation of an ordered retinotopic map in area 17.





**Figure 10: Blank corrected retinotopic maps from three mice with different genotypes**  
 (A) Wild type mouse, (B) heterozygous mouse, (C) knockout mouse. Note that not only in the wild type mouse but also in the heterozygous as well as in the knockout mouse there is a clear progression of the patch from map to map, indicating that a retinotopic map is present. The indices denote the stimulus position according to Figure 8B. Scale bars: 1mm.

Due to the small inter-animal variability of the maps, it is possible to average the maps across several animals from the same genotype (Figure 11). This was done by first aligning maps from different animals, using the centre of mass of the eight

strongest patches as reference points for translation and rotation. After this, the maps were averaged pixel by pixel.

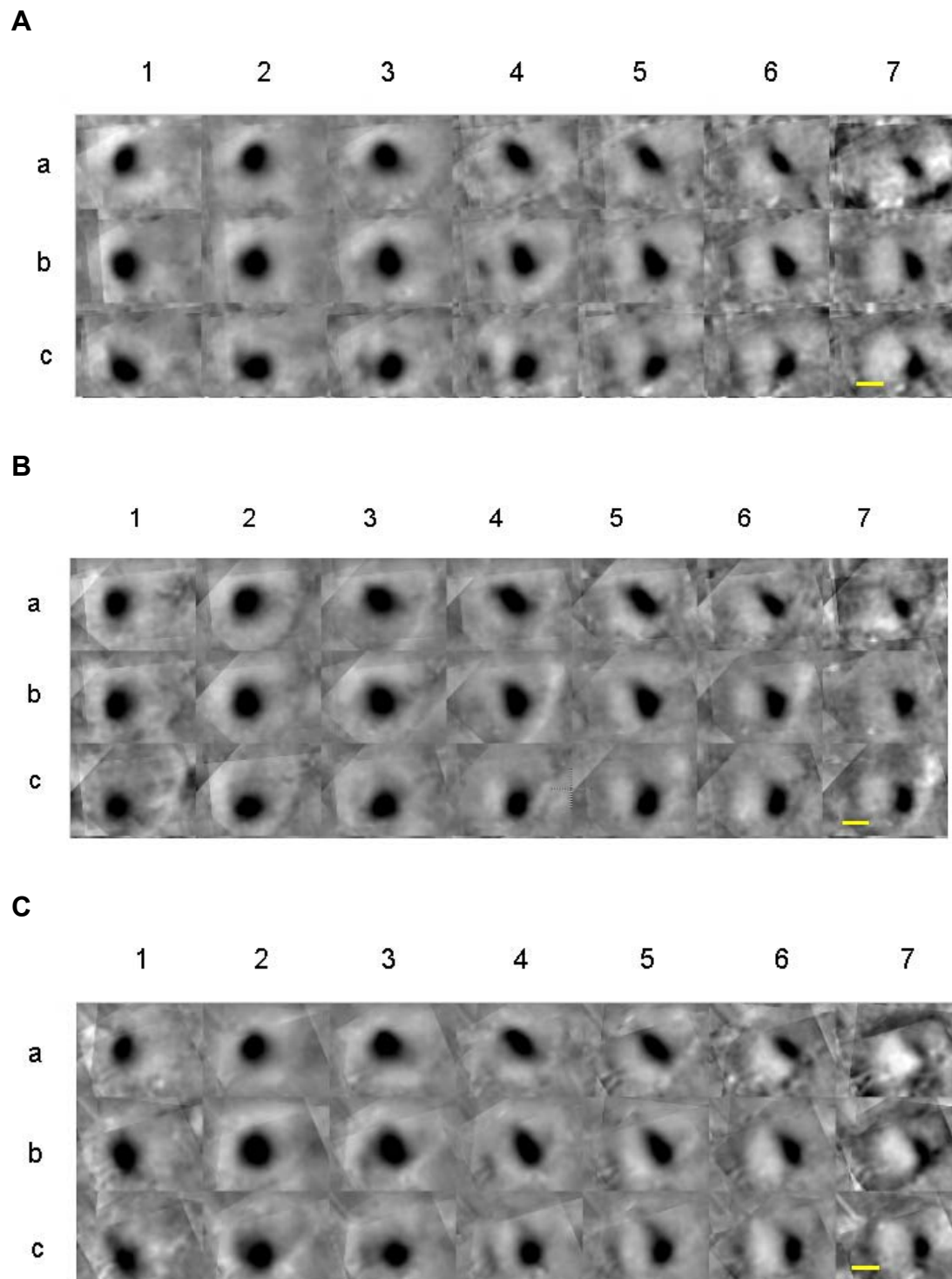


**Figure 11: Averaged single condition maps**

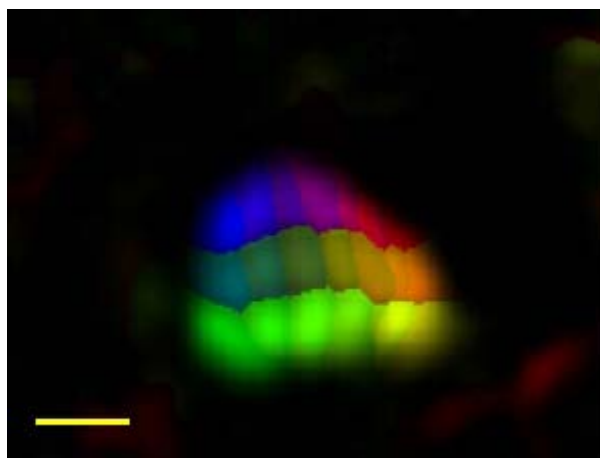
Single condition maps averaged across (A) 5 wild type mice, (B) 4 heterozygous mice and (C) 5 knockout mice. Note that there is an ordered retinotopic map in the wild type as well as in the heterozygous and the knockout animals. Conventions as in Figure 10. Scale bars: 1mm.

A qualitative examination of the characteristics of these averaged maps revealed some differences in the functional organisation of the visual cortex in the knockout mice, in particular a compression of the map medially in the cortex and a simultaneous expansion laterally.

As initial inspection of the maps in heterozygous mice showed only very modest changes I shall from now on limit the comparison to homozygous wild type and knockout mice.

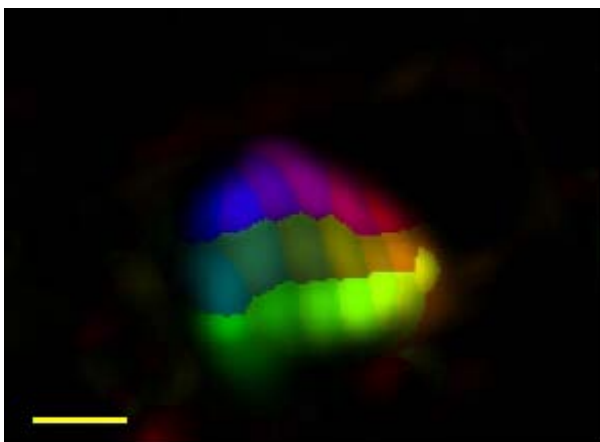
A suitable way to compare the general organisation of the visual cortex and the distribution of the patches is to examine the colour-coded retinotopic map of the two genotypes (Figure 12). This again reveals that, in the knockout mice, the map is compressed medially, that is in the cortical region representing the peripheral visual field.

**A**



averaged wild type mice

**B**



averaged knockout mice

**Figure 12: Colour-coded retinotopic maps in wild type (A) and knockout (B) mice**

Note the compression of the map in the medial part of area 17 in the knockout mice and the expansion in the more lateral part. Colour-code as described in Figure 9. Scale bars: 1mm.

A similar observation has been made by Schuett and colleagues in knockout mice lacking only one ephrin, ephrin-A5. Here, too, the map in area 17 showed a slight compression medially (Schuett et al, 2001). An equivalent result has been obtained by Prakash and colleagues in the barrel cortex (i.e. the part of the somatosensory cortex that represents the whiskers) of ephrin-A5 knockout mice, where the barrel map was found to be compressed medially and expanded laterally (Prakash et al., 2000).

As a first step to quantitatively compare the maps in both groups of mice I analysed the exact positions of the patches. This was done by calculating the centres of mass for each averaged patch. Figure 13 shows the patch distribution in wild type and knockout mice. In the latter, the closer spacing of patches medially in the cortex becomes evident again. Another noticeable feature is the longer, more narrow and somewhat less regular shape of the map in the knockout mice.

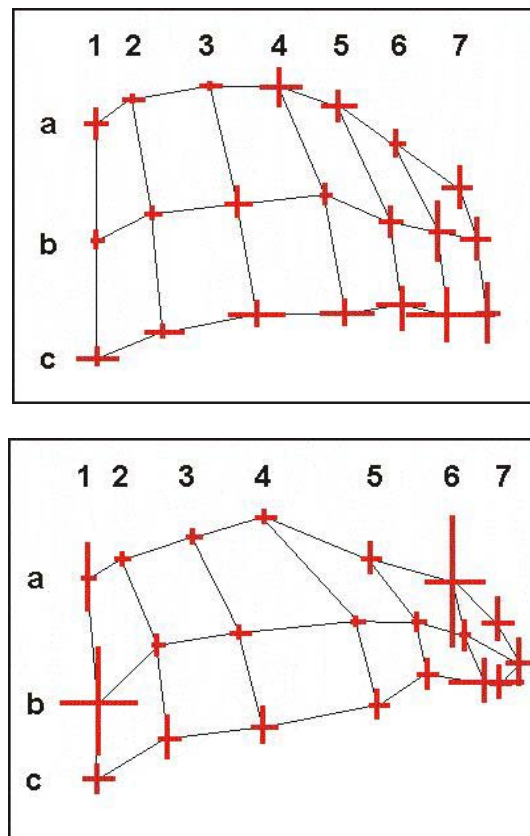


**Figure 13: Comparison of patch position**

Positions of the centres of mass of the patches in area 17 averaged across adult wild type (top) and knockout (bottom) mice. The numbers and letters denote stimulus position as in Figure 8. The lengths of the crossing bars indicate 1 SEM in vertical and horizontal direction. Note the slight compression of the cortical representation of the visual periphery (right) in the knockout mice. Moreover, the larger error bars in the knockout mice reveal a higher variability in patch position.

In wild type mice, the patches are arranged in almost parallel lines, both horizontally and vertically. In contrast, the averaged map of knockout mice appears less well organised, although overall neighbourhood relationships are clearly maintained.

In the plots shown above, the positions of the patches after averaging of the individual maps were compared. In order to test the degree of variability of patch positions within each genotype, the centres of mass were first determined for each individual map and only then averaged. Thus, one obtains the average position as well as a measure for the variability, which can be expressed as the standard error of the mean (SEM). The bars of the crosses denote the respective SEM in both horizontal and vertical directions for each patch. It is remarkable that in general, for many positions, the error bars are very small, once more indicating a high reproducibility between animals. Note, however, that the knockout mice show larger error bars, especially in the medial part of the cortex, indicating that patch positions vary more and are less predictable in these mice.

In summary, I found that an ordered retinotopic map exists both in wild type and in knockout mice. Although area 17 does show some distortions in knockout mice compared to wild type controls, these differences are not very strong. I therefore quantified certain features of these maps in more detail.

### **3.3 Quantitative characteristics of retinotopic maps in wild type and knockout mice**

Previous studies have shown that in ephrin-A5 knockout mice the axonal fibres migrating from the nasal part of the retina occupy a wider territory in their target area, the lateral geniculate nucleus (Feldheim et al., 1998). It is therefore conceivable that the patch sizes in the cortical target area are different in the mutant mice. Figure 14 depicts the patch sizes for wild type and knockout mice. The patch size was determined by thresholding the maximum intensity projection of the intrinsic signal 2.5 SD of the blank response above the mean of the blank.

While there was no significant difference between the two genotypes for any individual patch, it is obvious from these figures that in the knockout mice the lateral patches (those representing the central visual field) are larger while the medial ones (those representing the peripheral part of the visual field) are smaller. This matches the observation in the visual cortex of the knockout mice of a compression medially and an expansion laterally.

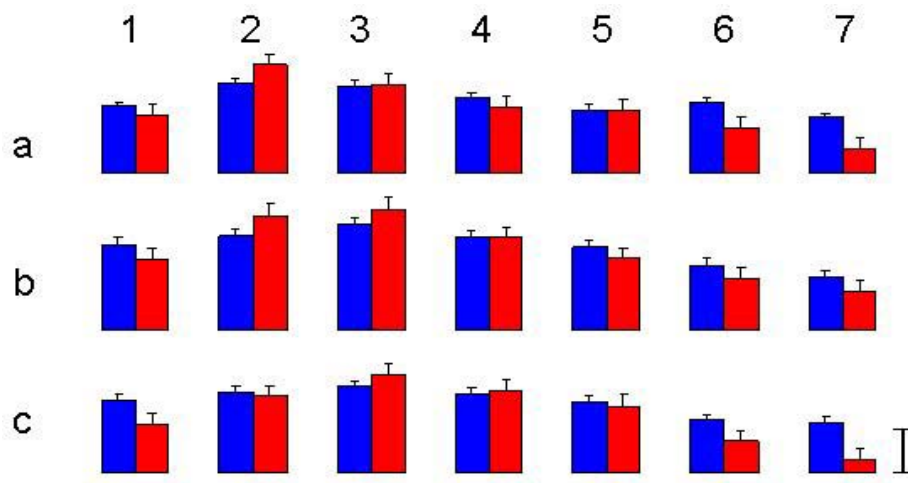


**Figure 14: Comparison of patch size**

The numbers and letters denote stimulus position as in Figure 8. Blue: wild type, red: knockout mice. Note that for knockout mice, patch sizes are smaller medially in the cortex (columns 6 and 7, representing stimuli in the periphery) and larger laterally in the cortex (columns 2 and 3, representing the centre of the visual field). Error bars indicate 1 standard error of the mean (SEM). Scale bar: 1.0 mm<sup>2</sup>.

To better illustrate the spatial distribution of the differences in patch size between the two genotypes, Figure 15 depicts the relative differences. There is a clear and systematic variation, with the knockout mice showing larger patches in the central visual field and smaller patches in the periphery.

These differences, however, are neither significant for all of the 21 patches taken together, nor for each individual patch. This may be due to the small sample size. Therefore, I divided the visual field into three regions: the “centre”, which is represented in the cortex by the columns 2 and 3, the “periphery”, represented by the columns 6 and 7, and the “middle” columns (4 and 5). When comparing the patch sizes between the different genotypes separately for each of these three regions, it turns out that the patches in that part of the cortex representing the central visual field are larger in the knockout mice, while they are clearly smaller in that representing the periphery. In order to verify this observation, I performed a two-factor ANOVA test that showed a significant difference in the sizes of the peripheral patches (i.e. columns 6 and 7) between wild type and knockout mice ( $p=0.00133$ ).

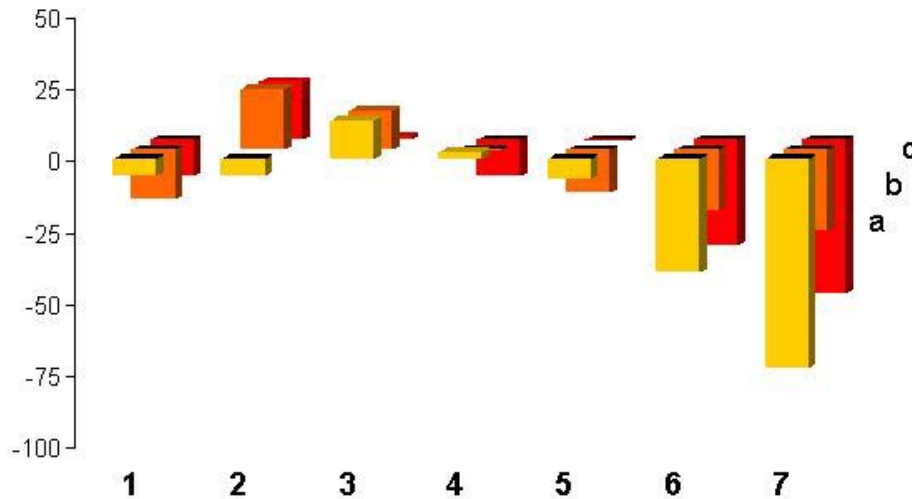


**Figure 15: Relative change in patch sizes (in percent) between wild type and knockout mice**

Relative changes in patch size between knockout and wild type mice. Positive values indicate larger patches in the knockout mice. Again, conventions as in Figure 8. In the central visual field (represented by columns 2 and 3), the patches of the knockout mice are slightly larger, while they are significantly smaller in the periphery (represented by columns 6 and 7),  $p = 0.00133$  (ANOVA).

In addition to differences in patch area, it is conceivable that the patches also differ in their shape. As it is difficult to quantify the exact shape of the patches, I chose to fit an ellipse to each patch. Thus, one can at least obtain a rough measure of the elongation of a patch as well as its spatial orientation in the visual cortex. The former can be described by determining the eccentricity of the fitted ellipse. The rounder the ellipse, the smaller the value for eccentricity; for a circle, the value would thus be 0.

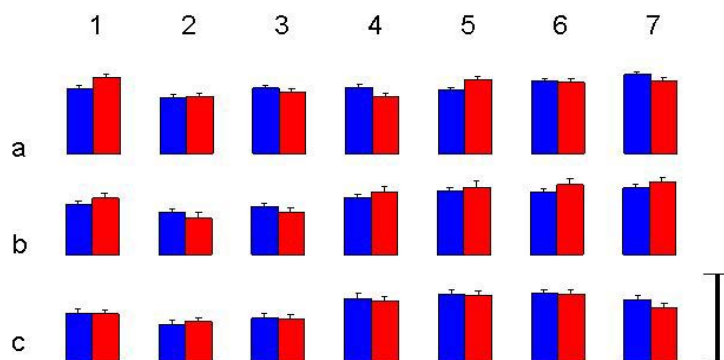


**Figure 16: Comparison of patch elongation**

As a simple measure to characterise the elongation of the patches, an ellipse was fitted to each patch. Lower values indicate less elongated patches. Conventions as in Figure 14. There is no difference between the two genotypes. Scale bar: eccentricity value of 1 (0 being a circle). Error bars indicate 1 SEM.

In terms of eccentricity, there seems to be hardly a difference between the two genotypes (Figure 16). Similarly, the orientation of the patches in the cortex is not different between wild type and knockout mice (Figure 17).

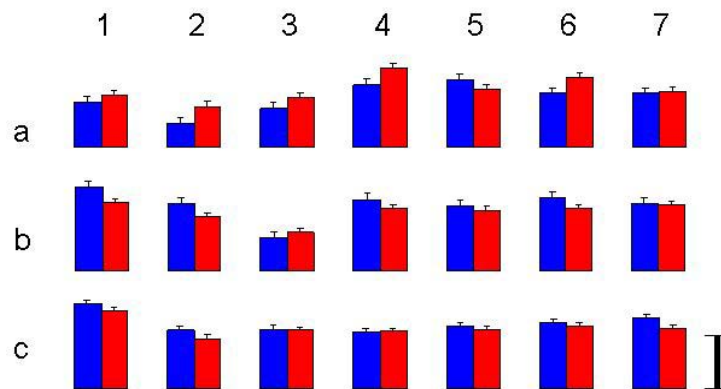


**Figure 17: Comparison of patch orientation**

The angle of the long axis of the ellipse fitted to the patch was measured relative to the midline of the brain (in counterclockwise direction). Conventions as in Figure 14. Patches in wild type and knockout mice overall have similar orientations. Scale bar: 45 degrees.

Thus, on this level of analysis, the shape and orientation of the patches show no difference between knockout and wild type mice.

So far I have quantified parameters, which were based on the notion of an already defined patch, not taking into account the actual signal intensity within this patch. From the single activity patches (i.e. Figure 10) it is clear, however, that the signal intensity can vary across the entire patch, and it might also differ between patches. Thus, in addition, I analysed the actual values of the integrated signal intensity of each patch in wild type and knockout mice (see Figure 18).

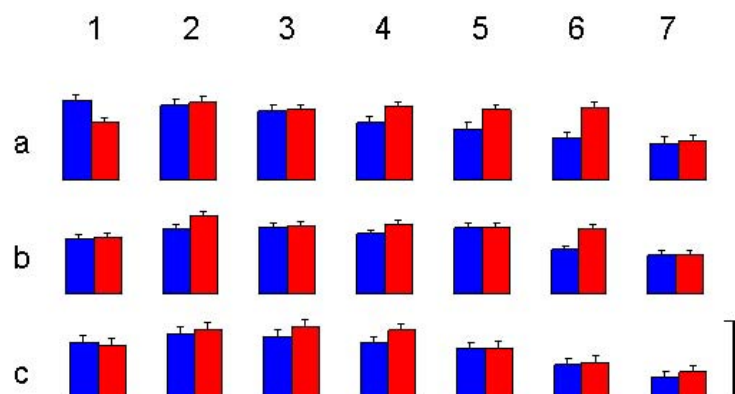


**Figure 18: Comparison of the integrated signal intensity of all patches**

Higher values indicate overall stronger light absorption, and thus a larger intrinsic signal. Again, conventions as in Figure 14. With this measure, too, there is no clear difference between the patches in wild type and knockout mice. Scale bar =1, arbitrary unit for reflectance change.

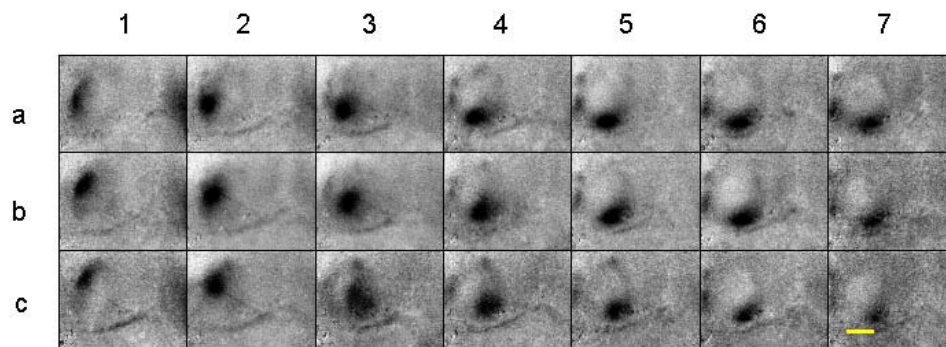


In summary then, my results show a slight distortion of the retinotopic map in area 17 in ephrin-A knockout mice, with a compression medially in the cortex, in the region where the peripheral visual field is represented. The patches themselves, however, do not seem to differ very strongly.

### 3.4 Retinotopic maps in young wild type and knockout mice

The retinotopic maps described above were all obtained from adult mice, aged 7 to 10 months. It is conceivable that, during development, mice lacking all A ephrins might have compensated this deficiency by other factors, such as neuronal activity or simply time. I therefore imaged the retinotopic maps of wild type and knockout mice of around two weeks of age, using the same stimuli and parameters as with the adult ones. At two weeks of age, the mice are very small and they are still suckling. This is probably the earliest possible age to obtain good quality maps with optical imaging.

**A**



**B**

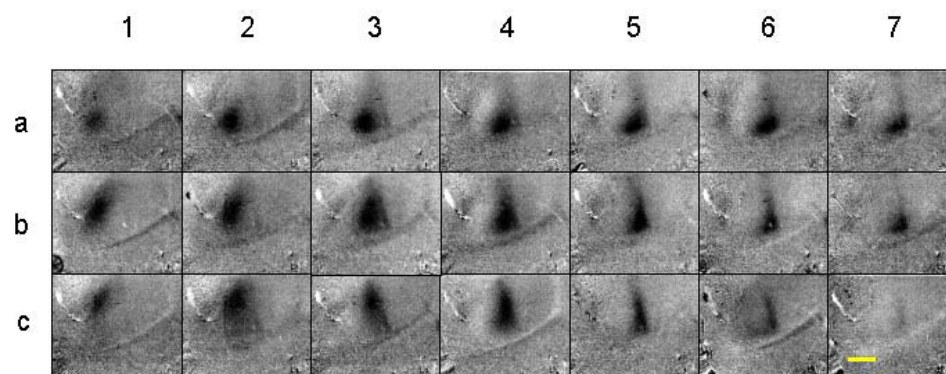


**Figure 19: Single condition maps in young wild type (A) and knockout (B) mice**

Blank corrected single condition maps from individual 2 week old mice. Note the ordered progression of the patch from map to map according to the change in stimulus position. Conventions as in Figure 10.

The average age of the wild type mice was 16 days ( $\pm 2$ ,  $n=4$ ) with an average weight of 8.5g. The knockout mice had an average age of 15.5 days ( $\pm 1.5$ ,  $n=4$ ) weighing on average 8.5g.

In general, these experiments show that a functional, well organised retinotopic map already exists in the visual cortex of such young mice.

As many features in the visual cortex of young mice, such as shape and size, are different from those in adult mice, and since there is also a higher signal to noise ratio in the young animals, it is not useful to directly compare the maps between the two age groups. The emphasis here will be on the difference between maps in young wild type and young knockout mice.

Figure 20 shows the retinotopic maps averaged across four wild type and four knockout mice.

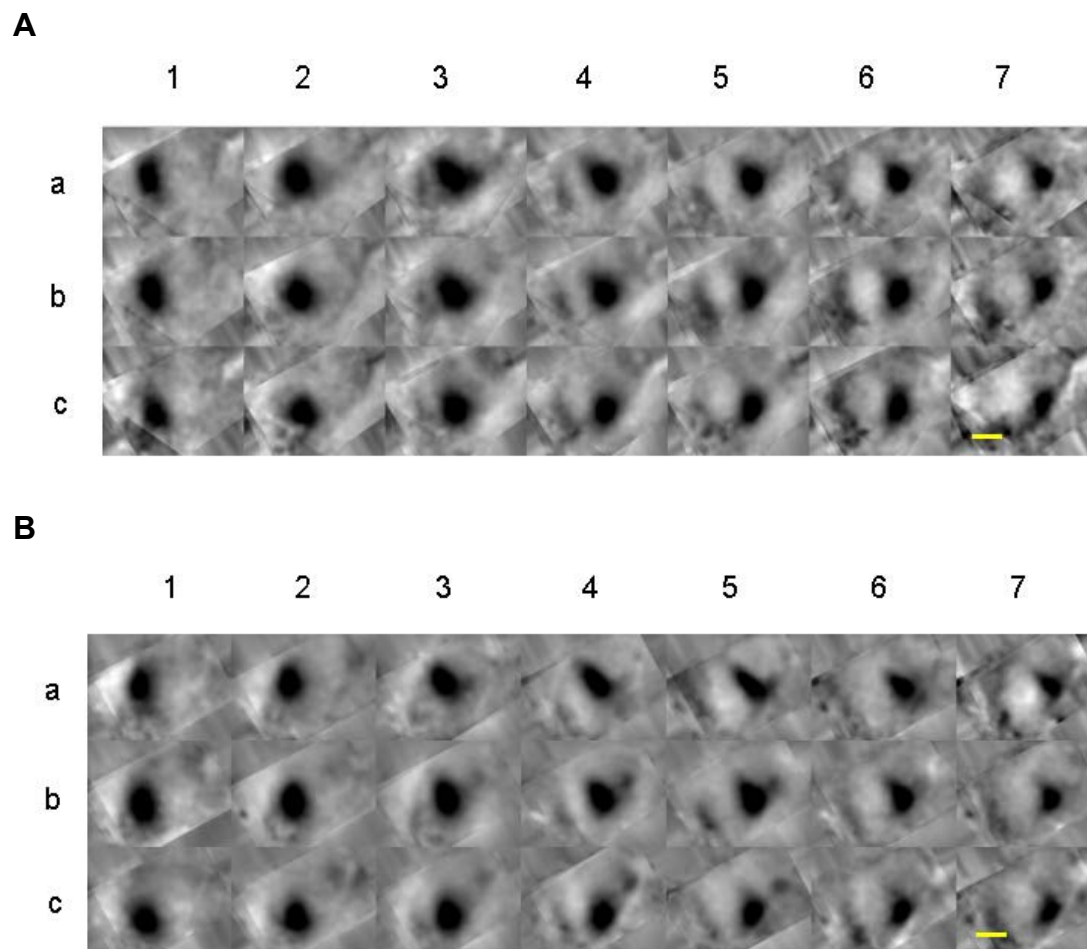


**Figure 20: Averaged retinotopic maps in young mice**

These maps were generated by averaging across four young wild type (A) and four young knockout mice (B). No conspicuous differences are visible. Conventions as in Figure 10.

Figure 21 displays the averaged colour coded retinotopic map of young wild type and knockout mice. Both maps show the overall familiar sequence of colours, but a clear difference in the overall shape is obvious.

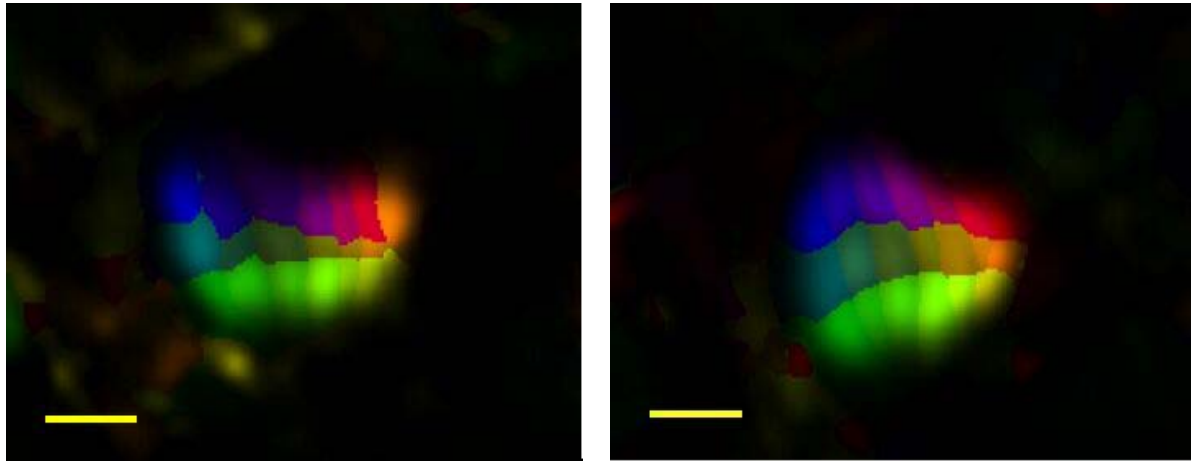


**Figure 21: Colour-coded map in young wild type (left) and knockout (right) mice**

Each colour corresponds to the stimulus position, which elicited the largest response at this point in the cortex. Note the different shapes of the maps. Conventions as in Figure 9. Scale bars: 1mm.

Examining the positions of the patches (Figure 22) reveals the overall preserved neighbour relationships in the maps of the wild type as well as the knockout mice. However, there is an obvious difference in the general shape of the map: the wild type mice have a map that is elongated in the lateromedial axis, while the map in the knockout mice is “rounder”.

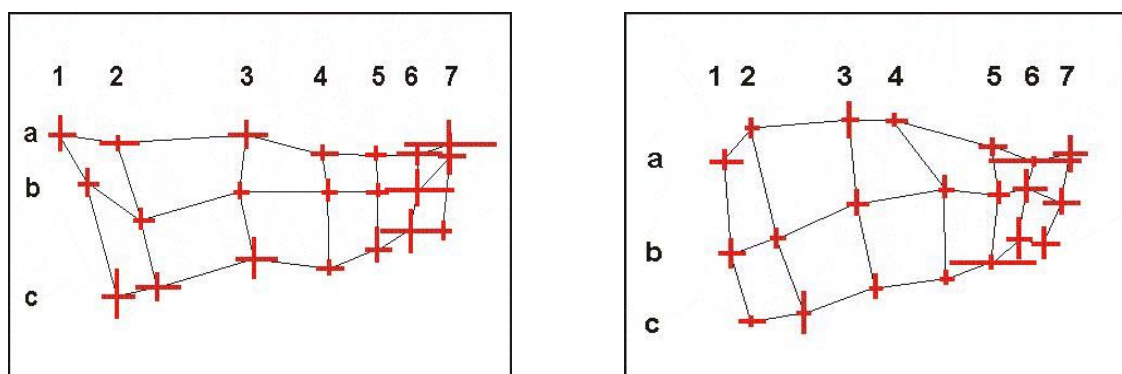


**Figure 22: Comparison of the patch position in young wild type and knockout mice**

Conventions as in Figure 13. The lengths of the crossing bars indicate 1 SEM in vertical and horizontal direction. The maps differ in shape: in transgenic mice (right panel), cortical regions representing the periphery (right) are compressed in the medio-lateral direction while the representation of more central parts of the visual field (left) is extended in the antero-posterior direction.

As a result, like in adult animals, the map of the knockout mice, compared to that in wild type mice, is compressed medially; however, this effect is not very strong.

The interindividual variation in patch position which is indicated by the crossing bars (1 SEM) is relatively low, supporting the notion that optical imaging is well suited to image retinotopic maps in young mice, too.

In the following, I will describe the results of the quantitative analysis of the maps in young mice. Figure 23 depicts the patch sizes of wild type and knockout mice. What stands out primarily, is the fact that the patches of the young knockout mice are *overall* larger. We are reminded that, in contrast, in the adult mice, the noticeable difference was *smaller* patch sizes in the knockout mice in the periphery of the visual field.

In a similar fashion as in adult mice, Figure 24 displays the differences in patch size between both genotypes in percent. This plot shows even more clearly, that, based on the averaged values, almost all patches are larger in knockout mice. Again, I performed a two-factor ANOVA test that shows that for all positions the patch sizes between young wild type and knockout mice are significantly different from each other ( $p < 0.00001$ ). These results could indicate that indeed a smaller degree of accuracy is present in the organisation of the retinotopic map at this early time point in development in the knockout mice, supporting the idea that there are mechanisms, which can compensate for initial mapping errors during maturation of the map.

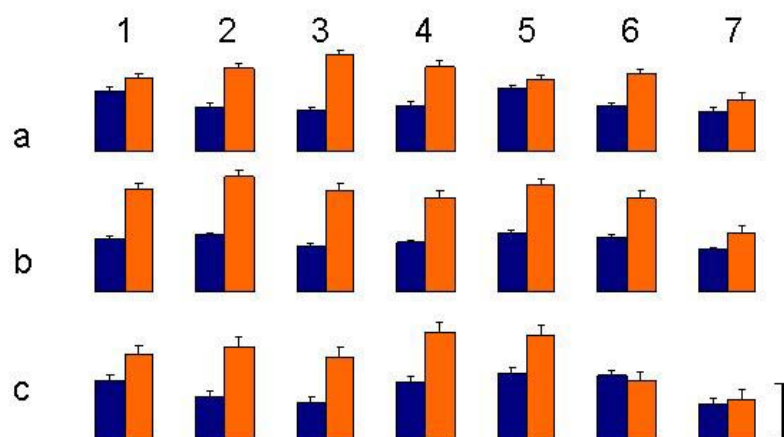


**Figure 23: Averaged patch size (and SEM) in young animals**

The numbers and letters denote stimulus position as in Figure 14. Blue: wild type, red: knockout mice. Note that the patches are overall larger in young knockout mice with a p-value of  $p < 0.00001$  (ANOVA). Scale bar =  $0.5 \text{ mm}^2$ .

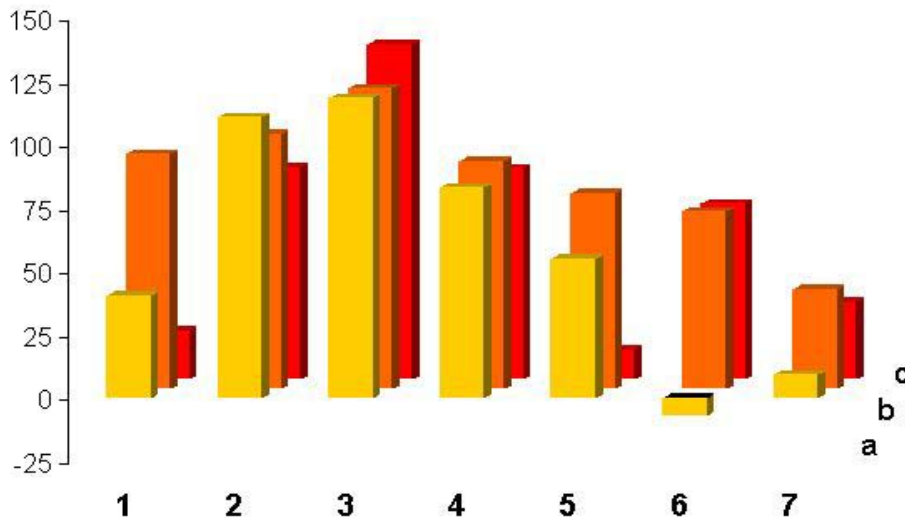


**Figure 24: Relative change in patch size (in percent) between young wild type and knockout mice**

Positive values indicate larger patches in the knockout mice. Conventions as in Figure 15.

As a next step to quantitatively compare maps in young mice, I analysed the patch shape (Figure 25) and patch orientation (Figure 26). The observations are similar to those made with the adult mice: no conspicuous differences are present between both genotypes.

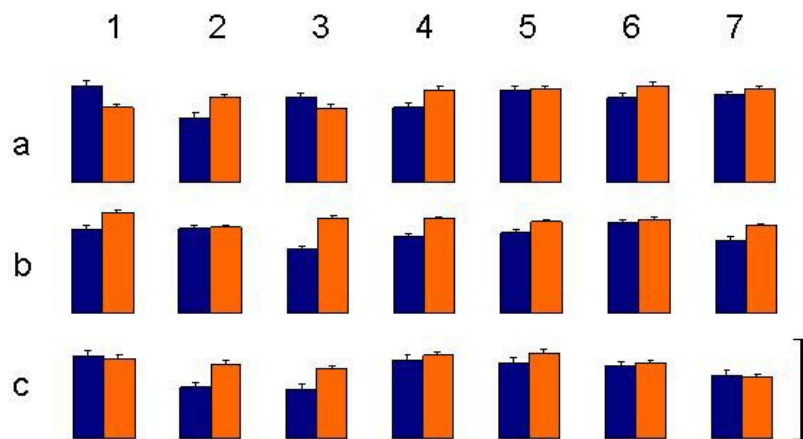


**Figure 25: Comparison of patch elongation in young mice**

Conventions as in Figure 14. Overall, patch elongation shows no clear difference between genotypes. Scale bar: eccentricity value of 1 (0 being a circle). Error bars indicate 1 SEM.

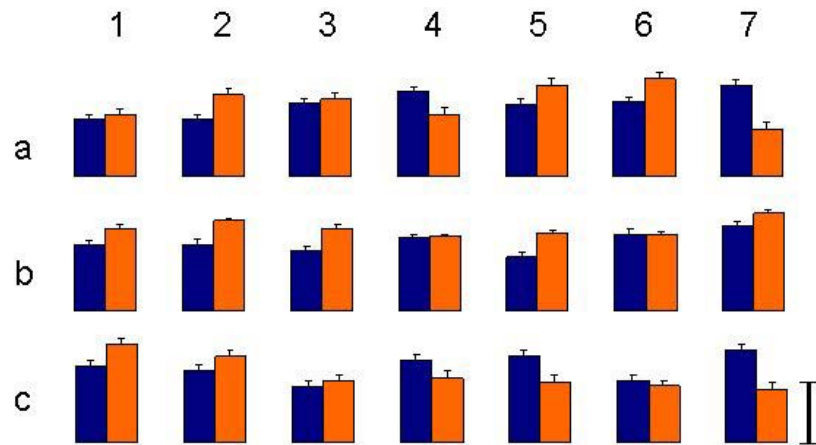


**Figure 26: Comparison of patch orientation**

Conventions as in Figure 14. No consistent differences are present. Scale bar: 45 degrees.

In summary, the absence of ephrin-A ligands leads to a slight distortion in the retinotopic map of the primary visual cortex of adult mice. From this we can conclude that the development of an ordered retinotopic map in the visual cortex does in part depend on the presence of ephrin-A ligands. But since a topographic map is clearly present in knockout mice, ephrin-As can not be the only group of molecules involved in the formation of this map. In addition, I found that the retinotopic map in young knockout mice is distorted more strongly. This implicates that later in development neuronal connections and topographic accuracy are refined by other mechanisms, such as activity-dependent processes.

## 4 Discussion

Previous work on the topographic projections from the vertebrate retina has established that ephrin-A ligands act as axon repellents and play key roles in directing axons to their proper target areas in the tectum (Cheng et al., 1995; Drescher et al., 1995; Nakamoto et al., 1996) and the thalamus (Feldheim et al., 1998).

Only few studies have asked the question whether ephrins also play a role in map formation in the neocortex. Based on expression patterns and *in vitro* assays, Vanderhaeghen and colleagues have demonstrated a distortion of the barrel cortex, the part of the primary somatosensory cortex that represents individual whiskers, in ephrin-A5 knockout mice (Vanderhaeghen et al., 2000). Prakash and colleagues have confirmed these results using optical imaging (Prakash et al., 2000). Both studies suggest a role for ephrin-A5 as a topographically specific “mapping label”. Gao et al. have shown complementary gradients of ephrin-A5 in the limbic cortex, and one of its receptors, EphA5, in the medial thalamic nuclei that project to it. Further, using their neurite outgrowth assay, they could demonstrate a repellent effect of ephrin-A5 on thalamic axon growth: medial thalamic neurons, which are EphA5 positive, did not project to the sensorimotor cortex that expresses high levels of ephrin-A5 (Gao et al., 1998). From these results it seems clear that ephrins play an important role for thalamocortical mapping, too.

In the current study I have used optical imaging to examine the role of the EphA receptor and ephrin-A ligand family in the development and organisation of the retinotopic map in mouse primary visual cortex. To this end, I compared maps in wild type mice with those in transgenic mice, which express and secrete a receptor body that binds and thereby neutralises all ephrin-A ligands.

The experiments lead us to four main findings or questions that shall be discussed in the following: I could demonstrate (4.1) that in transgenic mice functionally deficient for all ephrin-As, the overall retinotopy of area 17 is grossly normal, neighbourhood relationships in the retina being maintained in the cortex. However, I observed (4.2) a distortion in the shape of the retinotopic map in the visual cortex of the mutant mouse: the map is slightly compressed medially, where the peripheral visual field is represented, and expanded in the lateral region, which represents the central visual

field. This is essentially very similar to the observations made by Schuett et al. in ephrin-A5 knockout mice (Hübener et al., 2001) and raises the question (4.3), which role other ephrin ligands or even other guidance molecules play in thalamocortical axon guidance.

Using the same experimental paradigm in very young mice, I observed a much stronger phenotype (4.4). Overall, the patches were significantly larger in the knockout mice, possibly suggesting a lower degree of precision in map topography at this stage of development. This finding raises the interesting hypothesis that errors in guidance due to the absence of mapping labels may be corrected by other compensatory mechanisms over time.

#### **4.1 The retinotopic map in the primary visual cortex of ephrin-A knockout mice is grossly normal**

##### ***Do ephrin-A ligands play a role in the organisation and topography of cortical maps?***

A number of findings suggest indeed that ephrins play a role for map formation in the cortex: Imaging the somatosensory (barrel) cortex in ephrin-A5 knockout mice, Prakash and colleagues found moderate distortions in barrel sizes, with a contraction of barrels medially in the cortex (where ephrin-A5 is normally expressed at high levels) and an expansion of barrels laterally (Prakash et al., 2000).

Ephrin-A5 could be shown to be expressed in a gradient across the somatosensory cortex in mouse (Vanderhaeghen et al., 2000). Further, members of the EphA family are involved in the development of intracortical axonal connections (Castellani et al., 1998).

The presence of ephrins in the visual cortex is initially based on observations made in primates. Here, gradients of ephrin-A5 have been detected across embryonic visual cortex, with expression being high throughout the cortical plate in secondary visual cortex (V2), but restricted to the deepest strata in V1 (Sestan et al., 2001). Together with results from Gao and colleagues (1998), these data suggest a similar involvement of ephrins in the development of mouse visual cortex.

Also, experiments from this lab carried out by Sven Schuett, who imaged area 17 in ephrin-A5 knockout mice, indicate an important role for this ligand in the visual cortex: the retinotopic map in these mice, again, showed a compression in the



periphery that is comparable to the compression observed in the barrel cortex (Hübener et al., 2001).

Taken together, ephrin-A5 and possibly other ephrin-A ligands appear to be involved in the formation of topographic maps in the neocortex.

There are many ephrin-A ligands and EphA receptors, and a high degree of binding promiscuity is present within this receptor-ligand family (Flanagan and Vanderhaeghen, 1998). Feldheim and colleagues showed overlapping gradients for ephrin-A2 and ephrin-A5 in the tectum (Feldheim et al., 1998). Furthermore, the double ephrin-A2/A5 mutant revealed a deficit that was similar in phenotype but more severe than in either single mutant, suggesting a partial redundancy among the two ephrins in topographic mapping. It is therefore very probable that some ephrin-As compensate, in part, for others.

Taking further into account the wide variety of gradients of ephrins and Eph receptors that have been detected in several cortical areas (Gao et al., 1998; Vanderhaeghen et al., 2000; Sestan et al., 2001) it would be hard to elucidate the function of any single ephrin, let alone to infer a general function of all ephrins from the results obtained for a single one. Therefore, I chose to examine mice with a functional deficiency for *all* ephrin-As.

Intuitively, one would expect to see a stronger effect in these mice than that found in single ephrin knockout mice. However, qualitatively, my results do not differ much from those obtained by Sven Schuett in the ephrin-A5 knockout mice, raising the question why the simultaneous absence of all ephrin-As appears to have no greater influence than that of ephrin-A5 alone.

***Are the TIBFmyc mice really deficient of all ephrin-A ligands?***

The functional ablation of all ephrin-As in these mice is accomplished by the targeting of a cDNA coding for a receptor body, which should bind and thereby block all ephrin-As. Thus, in this mouse the strategy to delete a protein or a class of proteins is radically different from a more conventional knockout mouse. One might therefore ask whether all ephrin-A ligands are consistently ablated in this transgenic mouse.

Some important aspects of these TIBF-myc mice have been investigated and shall be discussed in the following.

The general effect of EphA5 receptor bodies has been demonstrated *in vivo* by intrahippocampal infusion of this protein. After such treatment these mice exhibited

impaired behavioural functions (Gerlai et al., 1999). Also, EphA receptor bodies have been shown to neutralize the repellent effect of ephrin-A ligands in stripe assays (Ciossek et al., 1998).

Lothar Lindemann (LL, personal communication) could demonstrate that, in TIBFmyc mice, neurons reliably secrete the receptor body and that it specifically binds and neutralises its ligands. However, currently, there is only indirect evidence that ephrin-As are actually blocked *in vivo*. This evidence is based on observations that the cortical phenotype in mice with a targeted deletion of one ephrin gene (ephrin-A5) is similar to that found in the TIBFmyc mice where the ephrin-A ligands are functionally blocked as described above. Additional evidence comes from examining the peripheral nervous system of E12 ephrin-A knockout embryos, where the number of arborisations was found to be increased in intercostal (afferent) nerves (LL, personal communication). Also, analysis of muscle innervation in E14 TIBFmyc embryos demonstrated a distinct increase in the number of arborisations.

The cDNA for the receptor body that blocks the A-ephrins was targeted to the locus encoding tau, a microtubule-binding protein. Thus, while the tau promoter is now used for the expression of the TIBFmyc gene, the tau gene itself is deleted. The tau locus was chosen because homozygous animals mutant for tau have been shown to be viable, fertile and display no gross morphological abnormalities in the central or peripheral nervous systems (Harada et al., 1994). Kerry Tucker and colleagues demonstrated that axon branching and outgrowth remain unchanged in tau-knockout mice (Tucker et al., 2001). Therefore, the effects that we see are unlikely to be caused simply by the disruption of the tau gene.

Another prerequisite for successful function is the right timing of the expression of this receptor antibody. Tau is expressed at high levels in all postmitotic neurons beginning at E 9.0; at E 10.75 expression is seen throughout the developing nervous system (Tucker et al., 2001; Binder et al., 1985). Retinothalamic as well as thalamocortical axons in the mouse reach their targets only several days later: The first retinal afferents have reached the optic chiasm by E14 (Godement et al., 1984) and thalamocortical axons do not start to grow out from the thalamus before E11 (Molnar and Blakemore, 1995). Thus, the receptor antibody is expressed well before thalamocortical mapping begins.

In summary, insertion of the receptor body construct into the tau gene seems to be very suitable for the generation of functional ephrin-A knockout mice. Furthermore, a

number of experiments demonstrate defects in the development of the peripheral nervous system in embryonic and early postnatal ephrin-A knockout mice, implying that there is indeed a deficiency for ephrin-A. However, whether this deficiency is as complete as in mice with a true deletion of all ephrin-A genes, is yet to be determined.

#### **4.2 Adult ephrin-A knockout mice show a distortion in the map of the primary visual cortex**

I found that in adult ephrin-A knockout mice the retinotopic map in area 17 is slightly compressed medially, where the peripheral visual field is represented, and that it is expanded in the lateral region, which represents the centre of the visual field (Figure 12, 13).

##### ***Are these effects due to a mapping defect in the thalamus, the cortex, or both?***

In their study investigating the connectivity and patterning of the somatosensory map in the cortex of ephrin-A5 mutant mice, Vanderhaeghen and colleagues, (2000) found no map distortions on the level of either brainstem or thalamus, while the map in the somatosensory (barrel-) cortex was malformed. Also, the observed ephrin-A expression patterns in brainstem and thalamus were not compatible with the observed distortions. Thus, they argue, ephrin-A5 is not important for topographic map formation at subcortical levels but rather plays a role for thalamocortical mapping and potentially for the patterning of intracortical connections (Vanderhaeghen et al., 2000).

However, in the visual system the situation might be different. In the lateral geniculate nucleus (LGN), the visual relay station in the thalamus that projects to the primary visual cortex, the absence of ephrin-A5 leads to incorrect mapping of retinal inputs (Feldheim et al., 1998). Retinothalamic axons originating in the nasal part of the retina, which usually form a dense arborisation close to the ventrolateral end of the LGN, form wider, less dense arborisations in the mutant mice, and they are also shifted away from their normal termination zone. Temporal axons form an additional smaller arborisation slightly displaced from the area in the LGN where they would usually terminate.

Based on this, there are two scenarios for retinotopic map development in the cortex of ephrin-A knockout mice: Either ephrin-As are directly involved in the guidance of thalamocortical axons. In this case, it would be difficult to predict the topographic organisation of the visual cortex. Alternatively, the (incorrect) map in the LGN is

“passed on” faithfully to the cortex, in which case any cortical distortions simply reflect those which are already present in the LGN. This alternative would suggest that the map in the cortex should closely correspond to that found in the LGN. According to Feldheim and colleagues (1998), in the ephrin-A5 knockout mouse nasal retinal axons migrating to the ventrolateral LGN, which thus contains a representation of the peripheral visual field, show wider arborisations. Thus, in the ephrin-A knockout mice we might anticipate cortical regions representing the periphery to show larger activated patches in response to visual stimulation.

Feldheim and colleagues (1998) also found that in the part of the LGN, which represents the central visual field, the majority of retinal axons project to the topographically correct sites, but that some project to a second, more ventral region. We should therefore expect to see ectopic activity patches in the corresponding region in the visual cortex of ephrin-A knockout mice.

Considering the two scenarios proposed above, my results meet neither of these expectations, since they show a compression of the cortical region that represents the peripheral field and an expansion of that representing the central field, with no apparent ectopic patches. However, we should take into account the different experimental paradigms used in these two sets of experiments. The retinothalamic projection was examined anatomically by injecting *Dil* into a very small region in the retina, thus making it possible to follow the projection of small groups of neurons. In my experiments, one visual stimulus simultaneously activates a much larger group of neurons, probably making it difficult to detect small changes, such as ectopic patches. This size was chosen as the optimal size to elicit a sufficient response at each position in the entire primary visual cortex including the very medial region, where the most peripheral part of the visual field is represented, and to ensure a uniform coverage of the entire visual field. Experiments are now under way in this lab that use smaller and fewer stimuli in order to try to detect more subtle changes.

Thus, while different experimental approaches were used to assess the retinothalamic and the thalamocortical projections, it seems that the defects on the level of the cortex cannot be explained easily. I therefore propose that the distortions of the retinotopic map in the cortex seen in ephrin-A knockout mice are mainly a consequence of an ephrin-A deficiency in thalamocortical – and, potentially, intracortical – connections, rather than a mere reflection of a malformation in the retinothalamic projection.

***Are ephrin-A ligands expressed in the neocortex?***

In order for the ephrin-A ligands to function as guidance molecules in the cortex, they need to be expressed in a specific way. The presence of ephrin-A ligands has been demonstrated in many areas of the neocortex (Gao et al., 1998; Vanderhaeghen et al., 2000; Sestan et al., 2001) and in a number of instances it was also found that they are arranged in gradients. Moreover, in the somatosensory (Vanderhaeghen et al., 2000) and the limbic (Gao et al., 1998) system it was shown that these cortical gradients match corresponding gradients of Eph receptors in the thalamic nuclei projecting to the respective cortical areas.

The expression of ephrin-A5 mRNA has also been demonstrated in the developing telencephalon: In the embryonic rat forebrain, ephrin-A5 is expressed in a distinct gradient across the dorsal half of the telencephalon, which corresponds to the developing neocortex (Mackarechtschian et al., 1999). Neurons in the dorsal thalamus express the receptors Eph A3 and Eph A4, and the graded expression of ephrin-A5 in the cortical subplate (the future white matter) mirrors the spatiotemporal gradient of cortical innervation by thalamic axons (Mackarechtschian et al., 1999).

The expression of ephrin-A ligands in a specific distribution across the visual cortex has been shown in primates. The detailed expression pattern of ephrin ligands in mouse visual cortex has not been established, but data from Vanderhaeghen and colleagues (2000) suggest that there is at least some expression of ephrin-A5 in the visual cortex. It has not been investigated whether the distribution is graded; such experiments are currently under way (Kostas Zarbalis, personal communication).

Taken together, the cortical expression pattern of ephrin-A ligands suggests that they play a role as axon guidance labels for the development of thalamocortical projections, most likely including the one into the visual cortex.

**4.3 Mice lacking all ephrin-A ligands show a similar cortical phenotype as ephrin-A5 knockout mice.*****Is ephrin-A5 the predominant mapping label in the visual cortex or are other ephrin-A ligands equally important?***

In the visual system, ephrin-A5 is probably the best studied of its class. Not only has its role been shown in the retinofugal projections (Cheng et al., 1995; Drescher et al., 1995; Nakamoto et al., 1996) but it has also been implied as an important mapping label in the thalamocortical pathways (Mackarechtschian et al., 1999). Gao et al.

(1998) propose this protein to be the major player in regulating thalamocortical projections.

To date, little is known about the role that other ephrin-A ligands and Eph receptors play in the retinofugal system and in the thalamus and its projections to the cortex, let alone for intracortical projections. Those ephrin-A ligands with an established relevance for the visual system shall be discussed in the following.

The presence of Ephrin-A2, for example, has been described in the retinotectal system, indicating a similar though also additive role to that of Ephrin-A5 (Feldheim et al., 2000).

Recently, a third ephrin, ephrin-A6, has been proposed to play a role for the developing visual system (Menzel et al., 2001): While ephrin-A2 and ephrin-A5 are predominantly expressed in the optic tectum, ephrin-A6 is highly expressed in the embryonic nasal retina of the chick and therefore does not show much homology with either of its cousin ligands. Rather, it is thought to activate EphA4 in nasal retinal cells, rendering these axons less sensitive to the ephrin repellent cues present on the posterior tectum.

The presence of various different EphA receptors seems to be essential, as shown for the EphA4 receptor in adult rat central nervous system: here, the distribution of this receptor is distinct from that of other EphA receptors, such that the function of EphA4 can hardly be compensated by other receptors (Martone et al., 1997).

Taken together, the abundant presence of ephrin-A ligands and EphA receptors that are expressed in various gradients across the entire central nervous system with different combinations of ligands and receptors used in different maps (Flanagan and Vanderhaeghen, 1998), together with their high binding promiscuity indicates a complicated and tightly intermingled dynamic of counterbalanced gradients and competition within the family. Thus, it would not be surprising if the absence of one single or of two complementary ephrins showed a stronger effect than that of all ligands at once.

In addition, despite the generally high binding promiscuity within this receptor-ligand family, it has been shown that an individual Eph receptor has a wide variation in affinity for different ephrins, and some interactions do not appear to trigger receptor activation (Brambilla et al., 1996). Therefore, a greater specificity may exist *in vivo* than suggested by the *in vitro* binding studies (O'Leary and Wilkinson, 1999).

Summarising the above, the family of ephrin-A ligands as a whole plays an important role in the development of cortical topography. Whereas the single ligands partially overlap in distribution and function, each of them is indispensable for the development of an accurate topographic map.

***The role of other ephrins for axonal guidance and map formation***

My observation that the general retinotopy in the primary visual cortex is still preserved, despite the absence of all ephrin-A ligands, could be explained by the existence of other repulsive or attractive guidance molecules with graded distributions in the cortex.

One important receptor ligand family that might complement the functions of ephrin-As is the closely related family of **ephrin-Bs** which are anchored to the membrane by a transmembrane domain (instead of the GPI-linkage of ephrin-A ligands). In the developing chick retina, the receptors EphB2 and EphB3 were shown to be expressed in a high ventral to low dorsal gradient and, consistent with this, ephrin-B1, the ligand for these receptors, is expressed in a high dorsal to low ventral gradient in the tectum (Connor et al., 1998). These results suggest that the ephrin-B family could be involved in establishing mapping in the dorsoventral dimension, in contrast to the anterior-posterior axis that seems to be determined by ephrin-A ligands.

The involvement of ephrin-B ligands has been shown in other systems, too. The connections between the two cortical hemispheres, for example, is disturbed through a targeted disruption of the ephB2 and the ephB3 gene. While mice deficient of EphB2 exhibit defects in path finding of anterior commissure axons (Henkemeyer et al., 1996), EphB3 mutants show defects in the formation of the corpus callosum (Orioli et al., 1996). This implies that EphB2 as well as EphB3 are both expressed and play an important role as topographic guidance labels in the neocortex.

Moreover, some ephrin-B proteins are also known to interact with EphA4 (Flanagan and Vanderhaeghen, 1998), see Figure 3, indicating a close cooperation between the two families and the possibility that one family can compensate for the other.

Taken together, ephrin-B ligands are present in many areas of the central nervous system and may play an important role as mapping labels. However, for more definitive statements, the spatial distribution of these ephrins needs to be determined by *in situ* hybridization.

***What about other guidance molecules?***

The ability of ephrins to act as guidance cues is a feature that is shared with two other recently identified classes of guidance molecules, the netrins and the semaphorins. It is conceivable that these molecules stand in when there is a lack of ephrins.

The **netrins** are a small family of secreted proteins that have been shown to play critical roles in guiding axons in the developing nervous system of many species including several vertebrates (Chisholm and Tessier-Lavigne, 1999). Netrins appear to be able to act as attractants on one group of axons while exerting a chemorepulsive action on another (Muller et al., 1996).

So far, netrins have not been shown to be involved in thalamocortical mapping. However, they do guide thalamocortical axons: Netrin-1 is expressed in the internal capsule, one of the major axon paths for thalamocortical axons and cortical efferents. Here, it acts as an attractant and growth promoter for dorsal thalamic axons as they extend towards the neocortex. Netrin-1 expression is not detected in the cortex itself, though (Braisted et al., 2000). In the thalamus, two groups of netrin-1 receptors have been described, one of which is expressed in the dorsal thalamus and acts as an attractant, the other, in parts of the ventral thalamus, acts as a repellent for netrin-1 expressing axons. Both *in-vitro* and *in-vivo* studies could show that netrin-1 stimulates dorsal thalamic axon outgrowth and provides a directional cue, i.e. a “growth corridor” for them. However, even though in netrin-1 knockout mice the axonal projection from the thalamus to the cortex is disorganised within and restricted to certain parts of the internal capsule, thalamocortical axons seem to exhibit normal area-specific targeting in the neocortex. Thus, netrin-1 is, clearly and expectedly, not solely responsible for the proper development of the thalamocortical projection. Rather, it is proposed to act together with other guidance cues to control axon path finding through the internal capsule and into the cortex (Braisted et al., 2000).

Another netrin, netrin-4, has been detected in the central nervous system, too. It is expressed in brain spinal cord, elements of the peripheral nervous system and in numerous neurons in the cerebral cortex (Yin et al., 2000). Its precise role as a mapping label, however, is still unclear.

Currently, the largest family of signaling molecules implicated in axonal guidance are the **semaphorins**, a class of molecules containing both secreted and membrane-bound proteins. While some semaphorins such as SemD have been shown to function as chemorepellents, inducing growth cone collapse of cortical axons and reducing axonal



branching, others such as SemE act as attractants for cortical axons (Bagnard et al., 1998). Different semaphorin genes are often co-expressed, suggesting that the specificity of innervation results from the multiple guidance cues acting synergistically. Furthermore, combined activities of the several semaphorins could confine afferent fibres to particular pathways or cortical layers by rendering surrounding regions inaccessible (Skaliora et al., 1998).

Taken together, a large number of molecules is implicated in mediating axonal guidance in the thalamus and cortex. Considering the extraordinary complexity of the thalamocortical connections it is not at all surprising that its structural and functional organization requires more than one family of genes. Rather it must be the combined activity of various guidance tags that lead the growth cone in the course of its migration toward its target area in the cortex.

#### **4.4 Young ephrin-A knockout mice exhibit a stronger phenotype than adult mice.**

The experiments presented here show slight distortions in the map of area 17 in adult ephrin-A knockout mice. These distortions are clearly stronger in young knockout mice, suggesting that initial errors are compensated during development.

##### *Which mechanisms influence and remodel the cortical map from birth to adulthood?*

The most important finding in the young ephrinA knockout mice is that the size of all patches together is significantly larger in the mutant mice, a difference, which is not seen between genotypes in adult mice. This may indicate a smaller degree of mapping accuracy in young ephrin-A knockout mice and implies that during later development these errors are corrected.

Which factors could contribute to the correction of mapping errors? Neuronal activity and visual experience have long been shown to be important for the development of maps in the visual cortex, like ocular dominance and orientation maps (Hubel and Wiesel, 1998). The influence of neuronal activity on the cortical retinotopic map is much less clear, though. However, studies in other parts of the visual system could demonstrate such effects. For example, Sretavan and colleagues were able to inhibit the formation of the eye-specific layers in the LGN by blocking activity in retinal ganglion cells with Tetrodotoxin (TTX). In these animals, they found retinotopic errors in the LGN, suggesting an activity dependent process to be responsible for the

precise branching patterns and location of axon terminal arborizations (Sretavan et al., 1988). Thus, during maturation, the normal stimulation of the retina by patterned visual inputs could initiate mechanisms in the ephrin-A knockout mouse, which would reduce functional defects in the cortical map and refine topographic accuracy. However, recent findings have triggered a discussion on whether it is really useful to think of a dichotomy of activity related versus molecular guidance molecules. Certain ephrin ligands and their receptors can be guidance molecules at the same time as being involved in synaptic plasticity: Dalva and colleagues (2000) could show that EphB2 receptors interact with NMDA receptors (glutamatergic receptors at excitatory synapses), and Grunwald and colleagues (2001) have shown that mice lacking EphB2 show defects in synaptic plasticity. This same Eph receptor has also been described as a mapping label in the retinotectal system (Flanagan and Vanderhaeghen, 1998). It thus seems that the same molecules that guide axons are also involved in activity related formation of neuronal connections.

When comparing the layout of the retinotopic maps it is somewhat surprising to see that the averaged map of the young knockout mice looks relatively similar to the map of the adult wild type and knockout mice, while the map of the young wild type mice looks different. Besides being on average slightly smaller, it is longer and narrower than all other maps. One interpretation for this could be the growth direction of the cortex during development. As overall brain size at that age is smaller, it is conceivable that during further development the overall shape of the cortex changes with growth. However, to fully answer this question, it would be necessary to closely observe the growth of the cortex and its change in shape over several time points during development.

#### **4.5 Conclusion**

The existence of ephrin-A ligands as molecular labels that guide the growth cone, and the graded expression of the Eph receptors that is complementary to their binding partners in the target area, give strong evidence for Sperry's 'chemoaffinity' theory in cortical map formation. However, although I was able to demonstrate an important role for the ephrin-A ligands and their receptors, this gene family cannot be solely responsible for the generation of the retinotopic map in the primary visual cortex.

Rather, my findings suggest that other molecules are also important for the striking accuracy of the retinotopic map in the cortex.

In addition, my results show that even after the initial wiring of the thalamocortical projection and long after birth, cortical maps can be refined by other mechanisms, the most likely one being the pattern and level of neuronal activity.

Still, many questions remain unanswered.

The distortions that I see in ephrin-A knockout mice, for example, enable us neither to define where nor when in the developing murine nervous system the observed malformations of the thalamocortical map take place. Is it a continuation of the distortions found in the lateral geniculate nucleus (LGN), is it a misguidance of the thalamocortical axons on their way through the radiatio optica to area 17, or is it in the primary visual cortex itself, where intracortical connections are made? Or need we go even further, to where the visual field is initially depicted, to the development of the eye, retina and optic tract? This question should be addressed in future experiments by using mice with a regionally specific deficiency of ephrin-As (Sauer and Henderson, 1988).

## Bibliography

- Bagnard D, Lohrum M, Uziel D, Puschel AW, Bolz J (1998) Semaphorins act as attractive and repulsive guidance signals during the development of cortical projections. *Development* 125: 5043-5053.
- Binder LI, Frankfurter A, Rebhun LI (1985) The distribution of tau in the mammalian central nervous system. *J Cell Biol* 101: 1371-1378.
- Bonhoeffer T, Grinvald A (1996) Optical imaging based on intrinsic signals: The Methodology. In: *Brain Mapping: The Methods* (Toga AW, Mazziotta JC, eds), pp 55-97. San Diego, CA: Academic Press, Inc.
- Braisted JE, Catalano SM, Stimac R, Kennedy TE, Tessier-Lavigne M, Shatz CJ, O'Leary DD (2000) Netrin-1 promotes thalamic axon growth and is required for proper development of the thalamocortical projection. *J Neurosci* 20: 5792-5801.
- Brambilla R, Brückner K, Orioli D, Bergemann AD, Flanagan JG, Klein R (1996) Similarities and Differences in the Way Transmembrane-Type Ligands Interact with the Elk Subclass of Eph Receptors. *Mol Cell Neurosci* 8: 199-209.
- Castellani V, Yue Y, Gao PP, Zhou R, Bolz J (1998) Dual action of a ligand for Eph receptor tyrosine kinases on specific populations of axons during the development of cortical circuits. *J Neurosci* 18: 4663-4672.
- Cheng HJ, Nakamoto M, Bergemann AD, Flanagan JG (1995) Complementary gradients in expression and binding of ELF-1 and Mek4 in development of the topographic retinotectal projection map. *Cell* 82: 371-381.
- Chisholm A, Tessier-Lavigne M (1999) Conservation and divergence of axon guidance mechanisms. *Curr Opin Neurobiol* 9: 603-615.
- Ciossek T, Monschau B, Kremoser C, Loschinger J, Lang S, Müller BK, Bonhoeffer F, Drescher U (1998) Eph receptor-ligand interactions are necessary for guidance of retinal ganglion cell axons in vitro. *Eur J Neurosci* 10: 1574-1580.

- Connor RJ, Menzel P, Pasquale EB (1998) Expression and tyrosine phosphorylation of Eph receptors suggest multiple mechanisms in patterning of the visual system. *Dev Biol* 193: 21-35.
- Drescher U, Kremoser C, Handwerker C, Loschinger J, Noda M, Bonhoeffer F (1995) In vitro guidance of retinal ganglion cell axons by RAGS, a 25 kDa tectal protein related to ligands for Eph receptor tyrosine kinases. *Cell* 82: 359-370.
- Feldheim DA, Kim YI, Bergemann AD, Frisén J, Barbacid M, Flanagan JG (2000) Genetic analysis of ephrin-A2 and ephrin-A5 shows their requirement in multiple aspects of retinocollicular mapping. *Neuron* 25: 563-574.
- Feldheim DA, Vanderhaeghen P, Hansen MJ, Frisen J, Lu Q, Barbacid M, Flanagan JG (1998) Topographic guidance labels in a sensory projection to the forebrain. *Neuron* 21: 1303-1313.
- Flanagan JG, Vanderhaeghen P (1998) The ephrins and Eph receptors in neural development. *Annu Rev Neurosci* 21: 309-345.
- Frisen J, Yates PA, McLaughlin T, Friedman GC, O'Leary DD, Barbacid M (1998) Ephrin-A5 (AL-1/RAGS) is essential for proper retinal axon guidance and topographic mapping in the mammalian visual system. *Neuron* 20: 235-243.
- Gao PP, Yue Y, Zhang JH, Cerretti DP, Levitt P, Zhou R (1998) Regulation of thalamic neurite outgrowth by the Eph ligand ephrin-A5: implications in the development of thalamocortical projections. *Proc Natl Acad Sci U S A* 95: 5329-5334.
- Gao PP, Zhang JH, Yokoyama M, Racey B, Dreyfus CF, Black IB, Zhou R (1996) Regulation of topographic projection in the brain: Elf-1 in the hippocamptoseptal system. *Proc Natl Acad Sci U S A* 93: 11161-11166.
- Gerlai R, Shinsky N, Shih A, Williams P, Winer J, Armanini M, Cairns B, Winslow J, Gao W, Phillips HS (1999) Regulation of learning by EphA receptors: a protein targeting study. *J Neurosci* 19: 9538-9549.
- Godement P, Salaun J, Imbert M (1984) Prenatal and postnatal development of retinogeniculate and retinocollicular projections in the mouse. *J Comp Neurol* 230: 552-575.

- Grinvald A, Lieke E, Frostig RD, Gilbert CD, Wiesel TN (1986) Functional architecture of cortex revealed by optical imaging of intrinsic signals. *Nature* 324: 361-364.
- Grunwald IC, Korte M, Wolfer D, Wilkinson GA, Unsicker K, Lipp HP, Bonhoeffer T, Klein R (2001) Kinase-independent requirement of EphB2 receptors in hippocampal synaptic plasticity. *Neuron* 32: 1027-1040.
- Harada A, Oguchi K, Okabe S, Kuno J, Terada S, Ohshima T, Sato-Yoshitake R, Takei Y, Noda T, Hirokawa N (1994) Altered microtubule organization in small-calibre axons of mice lacking tau protein. *Nature* 369: 488-491.
- Henkemeyer M, Orioli D, Henderson JT, Saxton TM, Roder J, Pawson T, Klein R (1996) Nuk controls pathfinding of commissural axons in the mammalian central nervous system. *Cell* 86: 35-46.
- Hubel DH, Wiesel TN (1998) Early exploration of the visual cortex. *Neuron* 20: 401-412.
- Hübener, M., Schuett, S., Zarbalis, K., Wurst, W., and Bonhoeffer, T. Optical imaging of the retinotopic map in the visual cortex of normal and ephrin-A5 knockout mice. *Soc.Neurosci.Abstr.* 27, 455. 2001h.  
Ref Type: Abstract
- Lindemann, L., Schnürch, H., Tucker, K. L., and Barde, Y. A. Testing a-ephrins as regulators of axonal elongation and branching during development. *Soc.Neurosci.Abstr.* 27, 598. 2001.  
Ref Type: Abstract
- Mackarehtschian K, Lau CK, Caras I, McConnell SK (1999) Regional differences in the developing cerebral cortex revealed by ephrin-A5 expression. *Cerebral Cortex* 9: 601-610.
- Martone ME, Holash JA, Bayardo A, Pasquale EB, Ellisman MH (1997) Immunolocalization of the receptor tyrosine kinase EphA4 in the adult rat central nervous system. *Brain Res* 771: 238-250.
- Menzel P, Valencia F, Godement P, Dodelet VC, Pasquale EB (2001) Ephrin-A6, a new ligand for EphA receptors in the developing visual system. *Dev Biol* 230: 74-88.

- Molnar Z, Blakemore C (1995) How do thalamic axons find their way to the cortex?  
Trends Neurosci 18: 389-397.
- Muller BK, Bonhoeffer F, Drescher U (1996) Novel gene families involved in neural  
pathfinding. Curr Opin Genet Dev 6: 469-474.
- Nakamoto M, Cheng HJ, Friedman GC, McLaughlin T, Hansen MJ, Yoon CH,  
O'Leary DD, Flanagan JG (1996) Topographically specific effects of ELF-1 on  
retinal axon guidance in vitro and retinal axon mapping in vivo. Cell 86: 755-  
766.
- O'Leary DD, Wilkinson DG (1999) Eph receptors and ephrins in neural development.  
Curr Opin Neurobiol 9: 65-73.
- Orioli D, Henkemeyer M, Lemke G, Klein R, Pawson T (1996) Sek4 and Nuk  
receptors cooperate in guidance of commissural axons and in palate  
formation. EMBO J 15: 6035-6049.
- Penfield and Rasmussen. The Cerebral Cortex of Man: A Clinical Study of  
Localization of Function.  
Ref Type: Generic
- Prakash N, Vanderhaeghen P, Cohen-Cory S, Frisen J, Flanagan JG, Frostig RD  
(2000) Malformation of the functional organization of somatosensory cortex in  
adult ephrin-A5 knock-out mice revealed by in vivo functional imaging. J  
Neurosci 20: 5841-5847.
- Sauer B, Henderson N (1988) Site-specific DNA recombination in mammalian cells  
by the Cre recombinase of bacteriophage P1. Proc Natl Acad Sci U S A 85:  
5166-5170.
- Schuett, S., Bonhoeffer, T., and Hübener, M. Mapping retinotopic structure and  
inhibition in mouse visual cortex with optical imaging. (2001).  
Ref Type: Unpublished Work
- Schuett S, Bonhoeffer T, Hübener M (2002) Mapping retinotopic structure in mouse  
visual cortex with optical imaging. J Neurosci 22: 6549-6559.

- Sestan N, Rakic P, Donoghue MJ (2001) Independent parcellation of the embryonic visual cortex and thalamus revealed by combinatorial Eph/ephrin gene expression. *Curr Biol* 11: 39-43.
- Skaliora I, Singer W, Betz H, Puschel AW (1998) Differential patterns of semaphorin expression in the developing rat brain. *Eur J Neurosci* 10: 1215-1229.
- Sperry, R. W. Visuomotor coordination in the newt (*Triturus viridescens*) after regeneration of the optic nerve. *Journal of Comparative Neurology* 79, 33-55. 1943.  
Ref Type: Journal (Full)
- Sretavan DW, Shatz CJ, Stryker MP (1988) Modification of retinal ganglion cell axon morphology by prenatal infusion of tetrodotoxin. *Nature* 336: 468-471.
- Tucker KL, Meyer M, Barde YA (2001) Neurotrophins are required for nerve growth during development. *Nat Neurosci* 4: 29-37.
- Tuzi NL, Gullick WJ (1994) eph, the largest known family of putative growth factor receptors. *Br J Cancer* 69: 417-421.
- Vanderhaeghen P, Lu Q, Prakash N, Frisen J, Walsh CA, Frostig RD, Flanagan JG (2000) A mapping label required for normal scale of body representation in the cortex. *Nat Neurosci* 3: 358-365.
- Walter J, Kern-Veits B, Huf J, Stolze B, Bonhoeffer F (1987) Recognition of position-specific properties of tectal cell membranes by retinal axons in vitro. *Development* 101: 685-696.
- Wilkinson DG (2000) Eph receptors and ephrins: regulators of guidance and assembly. *Int Rev Cytol* 196: 177-244.
- Yin Y, Sanes JR, Miner JH (2000) Identification and expression of mouse netrin-4. *Mech Dev* 96: 115-119.
- Zhang JH, Cerretti DP, Yu T, Flanagan JG, Zhou R (1996) Detection of ligands in regions anatomically connected to neurons expressing the Eph receptor Bsk: potential roles in neuron-target interaction. *J Neurosci* 16: 7182-7192.



## Summary

The mammalian cortex is arranged into a number of areas that represent our sensory, motor and cognitive functions. A characteristic feature of many sensory areas is their precise topographic organisation: in the same way as the “homunculus” in the somatosensory cortex represents the entire body surface, in the visual system retinal inputs are mapped topographically; i.e. spatial relationships in the visual field are maintained all the way to the primary visual cortex (area 17).

The formation of such maps has been shown to depend on specific guidance molecules that are recognised by outgrowing axons.

One major family of molecules implicated in axonal guidance and map formation are the ephrin ligands and their Eph receptors. These molecules have been shown to contribute to topographic mapping in several mammalian brain systems including the retinotectal and retinogeniculate projection.

Much less is known about mechanisms that are important for the formation of topographic maps in the cortex.

**This study** has investigated the role of ephrin-A ligands for the formation of the retinotopic map in the primary visual cortex of mice with optical imaging of intrinsic signals. Using grating stimuli presented at adjacent but non-overlapping positions within the visual field, I was able to visualise the retinotopic map in area 17 and resolve the pattern of retinotopic activity with high precision and reliability.

In order to examine the influence of ephrinA ligands on cortical map formation, I used transgenic mice with a functional ephrin-A deficiency. These mice have a cDNA inserted into their genome that codes for a receptor antibody, which blocks all ephrin-As.

I found an ordered retinotopic map in both wild type and transgenic mice, suggesting that other molecules or mechanisms apart from ephrin-A ligands are responsible for guiding thalamic axons to their target in the primary visual cortex.

However, I also detected some important differences between the two genotypes: in ephrin-A knockout mice, the cortical representation of the peripheral visual field is compressed while that of the central field is expanded.

Moreover, I applied the same paradigms to mice of about two weeks of age showing similar but evidently stronger effects in the young ephrin-A deficient mice, implying that initial errors in map formation can be corrected later in development. This observation suggests that the formation of topographic maps is not only regulated by genes that are expressed early in development, but that activity dependent neuronal plasticity plays a fundamental role, too.

## Zusammenfassung

Die **Großhirnrinde der Säuger** ist in eine große Zahl unterschiedlicher Areale unterteilt, die Sitz unserer sensorischen, motorischen und kognitiven Funktionen sind. Charakteristisch für viele sensorische Areale ist ihre sehr genaue topographische Organisation: So wie z.B. im somatosensorischen Kortex der „Homunculus“ die gesamte Körperoberfläche repräsentiert, sind auch im visuellen System die retinalen Eingänge topographisch organisiert, d.h. die räumlichen Beziehungen zwischen Punkten im visuellen Feld bleiben auf dem gesamten Weg von der Netzhaut bis zum primären visuellen Kortex (Area 17) erhalten.

Es konnte gezeigt werden, dass die Entwicklung solcher Karten durch die räumliche Verteilung von Wegfindungsmolekülen gesteuert wird, die von auswachsenden Axonen gelesen werden. Eine für die Lenkung von Axonen und die Entstehung topographischer Karten wichtige Molekülfamilie ist die der Ephrin Liganden und ihrer Eph Rezeptoren. Ihre Rolle ist insbesondere für die retinalen Projektionen ins Mittel- und Zwischenhirn etabliert. Viel weniger wissen wir darüber, welche Mechanismen für die Entstehung topographischer Karten im Kortex wichtig sind.

**In der vorliegenden Arbeit** habe ich die Rolle der EphrinA Liganden bei der Entstehung der retinotopen Karte im primären visuellen Kortex der Maus mit optischen Ableitungen von intrinsischen Signalen untersucht. Mit Hilfe visueller Stimuli, die an benachbarten aber nicht überlappenden Positionen im Gesichtsfeld präsentiert wurden, konnte ich die retinotope Karte in Area 17 mit hoher Auflösung sichtbar machen.

Um den Einfluss der Ephrin-A Liganden zu untersuchen, verwendete ich eine transgene Maus mit einer funktionellen Ephrin-A Defizienz. Bei dieser Maus beruht die Blockade aller A-Ephrine auf der Insertion einer cDNA in das Genom, die für einen Rezeptor-Antikörper kodiert, der an alle A-Ephrine bindet.

Sowohl in Wildtypmäusen als auch in diesen transgenen Mäusen konnte ich eine geordnete retinotope Karte ableiten, was zunächst darauf hinweist, dass neben den Ephrin-A Liganden auch andere Moleküle oder Mechanismen für die Lenkung der thalamischen Axone zu ihren Zielorten im visuellen Kortex verantwortlich sind.

Ich habe jedoch auch einige wichtige Unterschiede zwischen den zwei Genotypen gefunden: die kortikale Repräsentation des peripheren Gesichtsfeldes ist bei den Ephrin-A defizienten Mäusen komprimiert, während die des zentralen Gesichtsfeldes vergrößert ist.

Optische Ableitungen der retinotopen Karte im visuellen Kortex von jungen, etwa 2 Wochen alten Mäusen zeigten interessanterweise deutlich stärkere Effekte.

Dies legt nahe, dass initiale Fehler in der Karte im späteren Verlauf der Entwicklung korrigiert werden können. Diese Beobachtung weist darauf hin dass die Entstehung topographischer Karten nicht nur durch früh in der Entwicklung exprimierte Gene reguliert wird, sondern dass aktivitätsabhängige neuronale Plastizität ebenfalls eine wichtige Rolle spielt.

# Curriculum Vitae

**Name** Claire Johanna Creutzfeldt

**Date of birth** 17. April 1976

Abitur	06/1995	Theodor-Heuss-Gymnasium Göttingen
University	04/1996-04/1998	Preclinical years at Justus-Liebig-Universität Giessen, Germany
	04/1998	Physikum
	04/1998-06/2003	Clinical years at Ludwig-Maximilian-Universität München, Germany
	04/1999	1. Staatsexamen
	04/2001	2. Staatsexamen
	06/2003	3. Staatsexamen
clinical rotations		Internal medicine, RPAH, Sydney, Australia, October/November '95 Paediatric Oncology, University of Göttingen, March '97 Cardiology, Krankenhaus Bogenhausen, München, July '98 Gynecology & Paediatrics, La Paz, Bolivia, May/ June '99 Internal medicine, General Practice, Göttingen, March '00 Neurology, MGH, Boston, USA, Sept. '00
lab rotations		Dept. of Neurobiology, MPI für Biochemie, Göttingen, June '94 MPI für Hirnforschung, Frankfurt, July '97 Dept. of Neurological Surgery, Univ. of WA, Seattle, USA, August '00
MD-studies:		“The role of ephrinA for retinotopic map formation in mouse visual cortex – an Optical Imaging Study” Bonhoeffer lab, Max-Planck-Institute for Neurobiology, Martinsried, Germany, May '01-April '02
graduate program		Member of the DFG-Graduiertenkolleg „Sensorische Interaktion in biologischen und technischen Systemen“, May '01 -April '02
Praktisches Jahr:		1/3: Internal Medicine at Brigham & Women's Hospital and Mt Auburn Hospital, Harvard Medical School; April - July'02 2/3: Surgery at Chirurgische Klinik Nußbaumstr., Ludwig-Maximilian Universität München; August -November '02 3/3:Neurology at the National Hospital for Neurology & Neurosurgery, Queen Square, London, UK, December '02-February '03